Energy Conversion and Management: X 26 (2025) 100996

Contents lists available at ScienceDirect

Energy Conversion and Management: X

journal homepage: www.sciencedirect.com/journal/energy-conversion-and-management-x

Retrofitted long-range hydrogen aircraft: A viable path to sustainable aviation?

Saeed Rostami [a,b], Khodayar Javadi [a], Abbas Maleki [b,*]

[a] Department of Aerospace Engineering, Sharif University of Technology, Azadi Ave., Tehran, Iran
[b] Depatment of Energy Engineering, Sharif University of Technology, Azadi Ave., Tehran, Iran

ARTICLE INFO

Keywords:
CO_2 equivalent
Direct operating cost
Energy transition
Hydrogen aircraft
Long-range aircraft
Biofuel
Aviation emission

ABSTRACT

The aviation industry faces increasing pressure to decarbonize, yet long-range flights have limited alternatives due to the need for high-energy–density fuels. Hydrogen is a promising candidate, but its feasibility depends on selecting the optimal production pathway, addressing nitrogen oxides (NO_x) emissions, and managing hydrogen leakage. This study comprehensively evaluates six hydrogen production pathways for retrofitted long-range hydrogen aircraft, assessing their emissions, operating costs, and environmental-cost trade-offs. The results show that without NO_x mitigation, hydrogen-powered aircraft emit 8.6% to 58.6% more equivalent of carbon dioxide (CO_2eq) than Jet-A even under the most favorable pathway (renewable electrolysis, ERE). Additionally, hydrogen aircraft's direct operating cost is significantly higher, with ERE increasing costs by 91% in medium twin-aisle aircraft and up to 132% in very large aircraft. A NO_x sensitivity analysis indicates that at least 15% NO_x reduction is required for medium twin-aisle aircraft to achieve lower emissions than Jet-A, while larger aircraft need reductions of 60–75%. The Eco-Efficiency Index confirms that even with NO_x mitigation, hydrogen aircraft remain less cost-efficient than Jet-A. Furthermore, hydrogen leakage penalties are higher in ERE for long-range aircraft, highlighting additional sustainability challenges.

1. Introduction

Currently, long-range aircraft make up less than 20 % of the global commercial fleet, a share that is projected to remain relatively stable in the coming decades [1]. Despite their limited presence, these aircraft account for nearly 50 % of total aviation-related carbon emissions [2], where the aviation industry emits over a gigatonne of equivalent of carbon dioxide (CO_2-eq) annually, making it one of the key sectors requiring urgent decarbonization [3]. Despite long-range aircraft's small share in the global fleet and disproportionately high emissions, long-range aircraft remain indispensable to the aviation industry. Eliminating this class is not a viable option, as it plays a crucial role in global trade, business connectivity, medical transport, and overcoming geographical barriers. Additionally, long-range aircraft hold significant economic value, demonstrating strong market competitiveness compared to other aircraft classes [4]. A substantial portion of the aviation industry's $996 billion revenue in 2024 [5] is attributed to this sector, underscoring its economic importance. The fundamental challenge is whether the long-haul sector can achieve decarbonization without undermining its vital role in the aviation industry. Unlike short-range flights, which have multiple decarbonization pathways, including electrification [6–8], the long-haul sector has limited alternatives. The primary challenge is that any alternative fuel must possess a high energy density to sustain extended flight durations. Given this requirement, Sustainable Aviation Fuels (SAFs) [9–12] and hydrogen [3,13] emerge as the most viable options for reducing emissions in long-range aviation. Meanwhile, SAFs encounter several challenges, including land use requirements, high costs, and the inability to achieve true net-zero emissions [14]. Similarly, hydrogen faces obstacles such as the significantly higher cost in certain production pathways compared to fossil fuels, along with a lack of reliable data on engine-level emissions, particularly concerning nitrogen oxides (NO_x) formation and pure hydrogen leakages. While hydrogen adoption in short-range flights has generated optimism, with initiatives like Airbus' ZEROe project leading the way, the key question remains: Can retrofitted hydrogen aircraft enable truly sustainable long-range aviation?

Dray et al. assumed that NO_x emissions from hydrogen combustion would be comparable to those of kerosene fuel [15]. However, in a separate analysis, they indicated that hydrogen use could potentially reduce NO_x emissions by 28–35 %, highlighting the uncertainty and variability in emission estimates depending on engine design and

* Corresponding author.
E-mail address: maleki@sharif.edu (A. Maleki).

https://doi.org/10.1016/j.ecmx.2025.100996
Received 12 February 2025; Received in revised form 24 March 2025; Accepted 29 March 2025
Available online 4 April 2025

Nomenclature

Acronyms

ADP	aircraft delivery price
AGWP	absloute global warming potential
AIM	aviation ıntegrated model
ASK	available seat kilometer
BG	biomass gasification
CG	coal gasification
DOC	direct operating cost
EEG	electrolysis powered by the existing grid
ERE	electrolysis driven by renewable resources
GWP	global warming potential
MTOW	maximum takeoff weight
RTS	renewable thermal water splitting
SAF	sustainable aviation fuel
SMR	steam methane reforming
VLA	very large aircraft

Symbols

a	production rate
α_H	combined chemical and deposition lifetime
α_R	lifetime of the perturbation
tp	legnth of step emission
PL	payload
ϑ	NOx estimating parameter
η	fuel use estimating parameter
C	cost ($)
D	distance (km)
f_{ATC}	air traffic control parameter
$k_{LH2Engine}$	hydrogen engine complexity coefficient
LR	labor rate ($)
n_e	number of engine
n_{pilot}	number of pilot
n_{att}	number of flight attendant
p	price
C	conversion rate
H	time horizon
R	radiative forcing
R_a	interest rate
R_i	insurance rate
R_{s-a}	airframe spares rate
R_{s-e}	engine spares rate
RV	residual value
T	time (hour)
Th	thrust (lbs)
W	weight
γ_{tank}	gravimetric efficiency
P	Penalty factor

combustion conditions [12]. Other researchers found that hydrogen combustion could reduce NO_x emissions by up to 86 %. However, their study also indicated that water vapor emissions would increase by a factor of 4.3 [16]. Schenke et al. argue that the direct use of hydrogen in aviation can help mitigate environmental impacts [17]. However, Rostami et al. [3] demonstrated that, regardless of aircraft class, certain hydrogen production pathways alone are insufficient to achieve sustainable aviation. Their findings emphasize that without effective policies aimed at reducing emissions in the fuel production cycle, the overall climate benefits of hydrogen-powered aviation remain limited. Overall, various studies have recognized that hydrogen has the potential to reduce emissions [18,19]. Another emerging concern in the aviation industry regarding hydrogen adoption is the potential release of unburned hydrogen into the atmosphere during flight. This issue, first examined within aviation by Rostami et al. [3], has previously been studied in other industries [20,21]. Research has highlighted that hydrogen leakage may have effects similar to those of other greenhouse gases, such as CO_2 [22]. The impact of hydrogen emissions has become a growing concern, emphasizing the need to understand their indirect contribution to global warming. Bertagni et al. highlight that while hydrogen is a promising low-emission fuel, its leakage can reduce hydroxyl radicals (OH), slowing the breakdown of methane (CH_4) and increasing its atmospheric levels. They emphasize minimizing hydrogen leakage to prevent unintended climate impacts [23]. Hydrogen also reacts with ozone (O_3), though its reaction is thermodynamically more favorable compared to its interaction with hydroxyl radicals [24].

The literature review highlights a significant gap between policymakers and researchers regarding the feasibility of achieving sustainable long-range aviation using hydrogen. Based on the available data, it appears unlikely that long-haul retrofitted hydrogen-powered aircraft can achieve lower economic and environmental impacts compared to fossil fuels. This is primarily due to three key uncertainties: limited data on NO_x formation during hydrogen combustion, a lack of comprehensive life-cycle assessments of various hydrogen production pathways, and insufficient knowledge about pure hydrogen leakage and its role in methane oxidation, ozone formation, and stratospheric water vapor. To address these uncertainties, this study first conducts a baseline evaluation of emissions and direct operating costs (DOC) for retrofitted hydrogen-powered long-range aircraft. It then assesses the feasibility of achieving emissions comparable to fossil fuel aircraft under various NO_x reduction scenarios. A comprehensive analysis is carried out on six hydrogen production pathways, considering their greenhouse gas emissions, economic viability, and technological feasibility across different regions. Unlike our previous study [3], which assessed carbon emissions at a macroscopic level, focusing on anticipating the total emissions from the entire aviation sector up to 2050, the current research investigates hydrogen-related emissions at the engine level for specific aircraft classes. This engine-level analysis allows us to explicitly assess the contributions and impacts of small, medium, large twin-aisle, and very large aircraft individually. Thus, the current work provides detailed insights into how different aircraft classes influence hydrogen-related emissions and environmental implications, which were not examined in our earlier broader-scope assessment. Additionally, this study explores the less-examined issue of hydrogen emissions and their potential atmospheric consequences. Overall, the primary objectives of this study are multifaceted and are as follows:

- Evaluating emissions and direct operating costs of retrofitted hydrogen-powered long-range aircraft in comparison to fossil-fuel-powered aviation.
- Assessing the impact of NO_x reduction strategies on the sustainability of hydrogen aviation.
- Analyzing life-cycle emissions across six hydrogen production pathways to determine their viability for aviation decarbonization.
- Investigating the atmospheric effects of hydrogen leakage, including its role in methane oxidation, ozone formation, and stratospheric water vapor.
- Providing insights for policymakers and industry stakeholders on the feasibility of hydrogen as a long-term solution for sustainable long-haul aviation.

The rest of the paper is organized as follows: Section 2 introduces the problem statement, while Section 3 details the methodology. Section 4 presents the model validation, followed by the results in Section 5, and

Section 6 concludes the paper.

2. Problem statement

The transition to retrofitted long-range hydrogen aircraft as a replacement for fossil-fuel-powered aviation presents several challenges, particularly regarding emissions and operational feasibility. Two critical concerns hinder the widespread adoption of hydrogen propulsion in long-range aircraft. First, there is a lack of accurate and reliable data on NO_x emissions at the engine level when burning hydrogen. Since NO_x formation is highly dependent on combustion conditions, existing data from kerosene-based engines is often used as a reference [15], but they may not accurately reflect the actual emissions from hydrogen propulsion. A key issue in evaluating the environmental benefits of hydrogen-powered long-range aircraft is determining the necessary level of NO_x emission reduction to make hydrogen a viable alternative to conventional fossil fuels. If NO_x emissions can be mitigated under different reduction scenarios, how significant would the environmental advantages be compared to kerosene-powered aircraft? This question is crucial for assessing whether hydrogen propulsion can contribute to the long-term sustainability of aviation. To address these uncertainties, the study is conducted in two main stages. First, a baseline assessment of both emissions and direct operating costs is performed for retrofitted hydrogen aircraft. This establishes a comparative reference with Jet-A-powered aviation. Second, a scenario-based analysis evaluates the feasibility of achieving sustainable long-range hydrogen aviation, particularly under different NO_x reduction strategies. On the other hand, a sensitivity analysis has been performed to evaluate the impact of variations in cost and emissions associated with the hydrogen production pathway.

Second, there is the risk of pure hydrogen release into the environment during various stages of storage, transportation, and combustion. The climatic effects of hydrogen leakage remain an area of ongoing research, as leaked hydrogen can contribute to indirect greenhouse gas effects by altering atmospheric chemistry. Therefore, retrofitted hydrogen-powered aircraft produce not only water vapor and nitrogen oxides but also significant amounts of unburned hydrogen, as illustrated in Fig. 1. Once released into the atmosphere, hydrogen undergoes complex oxidation reactions, which have both direct and indirect climate effects. A substantial 70 % to 80 % of the emitted hydrogen is absorbed by soil microbes through bacterial uptake and diffusion. The remaining 20 % to 30 % reacts with hydroxyl radicals (OH), triggering a series of chemical reactions that increase greenhouse gas concentrations in both the troposphere and stratosphere, ultimately contributing to global warming [20]. In the troposphere, hydroxyl radicals (OH) play a key role in breaking down methane, a major greenhouse gas. When hydrogen reacts with OH, it reduces their availability, prolonging methane's atmospheric lifespan, which accounts for nearly 50 % of hydrogen's indirect warming effect. Additionally, hydrogen oxidation generates hydroperoxyl radicals (HO_2), which contribute to higher

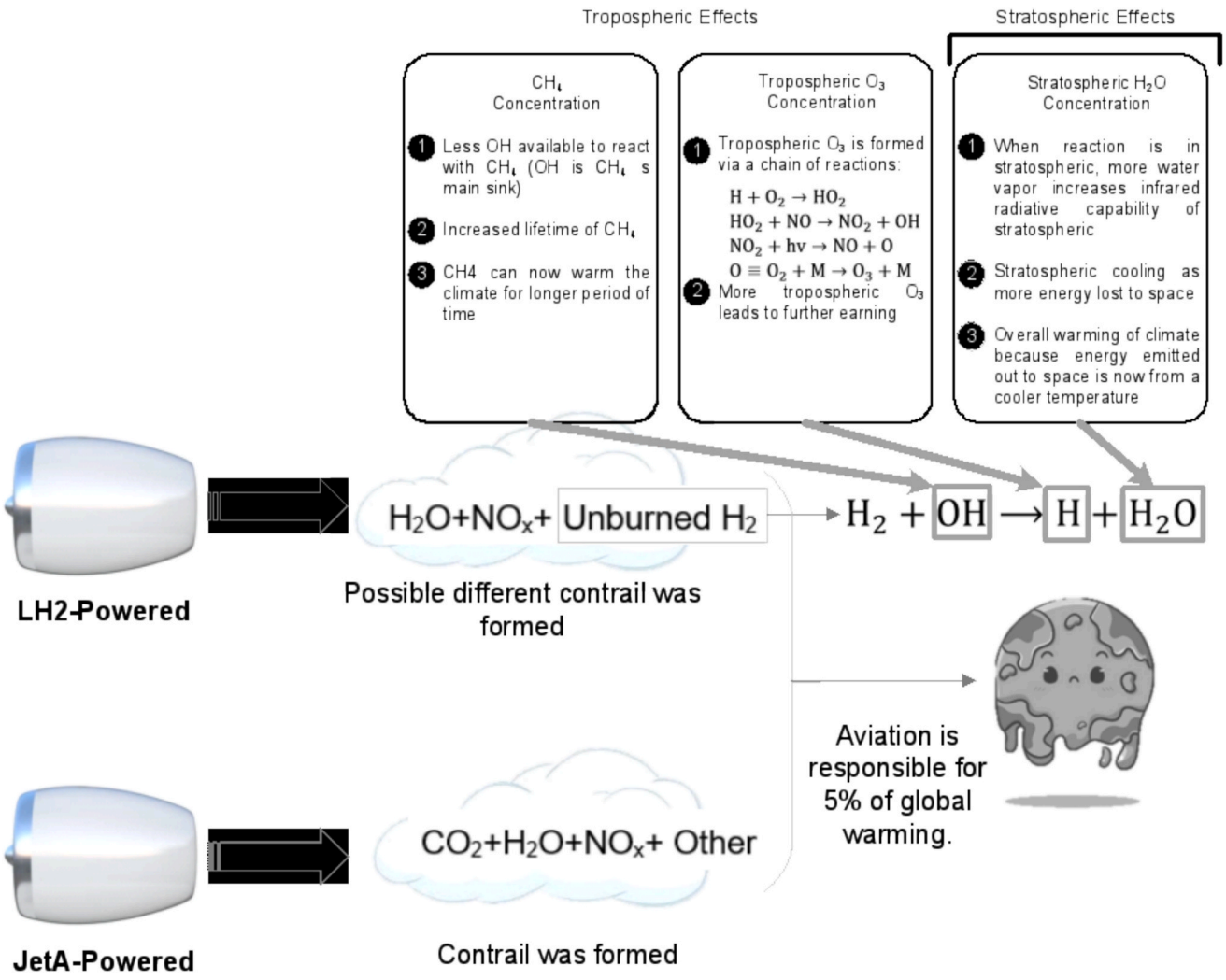

Fig. 1. Consequences of hydrogen oxidation on atmospheric greenhouse gas warming and concentrations.

tropospheric ozone levels, responsible for around 20 % of hydrogen's total warming impact [25]. In the stratosphere, increased hydrogen oxidation raises water vapor concentrations, enhancing infrared radiation absorption. This process leads to stratospheric cooling, which paradoxically warms the lower atmosphere by allowing more infrared energy to penetrate. This indirect effect accounts for approximately 30 % of hydrogen's total climate impact [26].

Given the two major challenges associated with retrofitted hydrogen-powered long-range aircraft—namely, NO_x emissions and the release of unburned hydrogen—this study aims to address both issues through a comprehensive evaluation framework. First, it seeks to identify an optimal NO_x reduction scenario that could make hydrogen-powered aviation environmentally competitive and support the transition toward sustainable air transport. This involves analyzing various NO_x mitigation levels and their impact on overall CO_2-equivalent emissions, determining the threshold at which hydrogen aviation can outperform conventional Jet-A fuel in climate terms. Second, the study quantifies the impact of unburned hydrogen emissions, which are often overlooked in conventional assessments. By incorporating net hydrogen leakage into the climate impact calculations, a penalty factor is introduced to reflect the indirect effects of hydrogen in the atmosphere. Ultimately, by integrating these two factors—NO_x reduction potential and hydrogen leakage penalties—the study aims to provide a holistic assessment of the viability of retrofitted hydrogen-powered aviation and its long-term sustainability.

3. Methodology

This study employs a comprehensive, multi-dimensional methodology to assess both the environmental and economic impacts of integrating hydrogen as an alternative aviation fuel. The first two sections focus on hydrogen leakage and its environmental consequences, incorporating detailed emission models to evaluate hydrogen's impact on atmospheric pollutants. From an economic perspective, the methodology utilizes a detailed cost modeling framework to assess the DOCs associated with retrofitted hydrogen-powered aircraft, considering factors such as fuel expenses, infrastructure modifications, and maintenance. Additionally, specialized performance models are integrated to address the design challenges of hydrogen storage within aircraft. These models evaluate the weight, volume, and structural implications of onboard hydrogen tanks, which influence aircraft efficiency, operational range, and payload capacity. By combining these environmental and economic assessments, the study provides a holistic evaluation of the feasibility and trade-offs involved in adopting hydrogen aviation technology.

3.1. Hydrogen production pathways

To ensure a comprehensive environmental and economic analysis, six hydrogen production pathways were selected based on their technical feasibility and potential for large-scale adoption. These pathways were chosen to represent a diverse range of energy inputs, including renewable power, natural gas, biomass, coal, and thermal energy, allowing for a comparative assessment of their sustainability and practicality. Table 1 provides an overview of the well-to-tank (WTT) emissions for each of the six hydrogen production methods, based on a comprehensive review study by Rostami et al. [3].

Table 1
Summary of the Well-to-tank (WTT) emissions for the main hydrogen production pathways.

Pathway	Full name	WTT (kg CO_2eq/kg H_2)	Ref.
SMR	Steam Methane Reforming	10.46	[3]
BG	Biomass Gasification	23.20	[3]
CG	Coal Gasification	21.07	[3]
EEG	Electrolysis using grid electricity	27.64	[3]
ERE	Electrolysis powered by renewable energy	1.92	[3]
RTS	Renewable Thermal Water Splitting	1.31	[3]

3.2. Hydrogen leakage factors

Examining the factors affecting hydrogen emissions at different stages of the value chain is crucial for understanding its environmental impact. This section expands on previous studies and assumes that 10 % of hydrogen escapes into the atmosphere without undergoing combustion [20]. Drawing upon findings from [21], This study assesses hydrogen leakage rates at 0.31 % for storage tanks at production sites and 0.03 % for airport storage facilities. Notably, hydrogen losses during transportation from production sites to airports are assumed to be insignificant. Instead of introducing new assumptions about pure hydrogen emissions during production, this research relies on findings from previous studies.

3.3. Hydrogen global warming potential

Unlike other greenhouse gases, hydrogen does not contribute to radiative forcing directly; instead, its impact on climate change is entirely indirect [26]. As discussed earlier, when hydrogen is released into the atmosphere, it triggers a series of chemical interactions that influence greenhouse gas concentrations. To quantify these effects, this study applies the Absolute Global Warming Potential (AGWP) equations formulated by Warwick et al. [20]. These equations are derived from chemical-climate modeling experiments specifically designed to evaluate hydrogen's climatic influence [20]. The AGWP equations account for three key components:

- AGWP1 represents the radiative forcing caused by the initial chemical disturbance following a step emission.
- AGWP3 describes the decay of this disturbance over time.
- AGWP2 accounts for residual chemical effects that persist in the atmosphere after emissions cease.

A critical aspect of assessing hydrogen's warming potential is selecting an appropriate time horizon. Given CO_2's long-term atmospheric presence, this study applies GWP-100, using the following equations:

$$AGWP_1 = Ra\alpha_R\alpha_H C\left[tp - \alpha_R\left(1 - exp\left(\frac{-tp}{\alpha_R}\right)\right) - \left(\frac{\alpha_H}{\alpha_H - \alpha_R}\right)\left(\alpha_H\left(1 - exp\left(\frac{-tp}{\alpha_H}\right) - \alpha_M\right)\left(1 - exp\left(\frac{-tp}{\alpha_R}\right)\right)\right)\right] \quad (1)$$

$$AGWP_2 = \frac{Ra\alpha_R\alpha_M^2 C(1 - exp\left(\frac{-tp}{\alpha_R}\right))}{\alpha_H - \alpha_R}\left[\alpha_H\left(exp\left(\frac{-tp}{\alpha_H}\right) - exp\left(\frac{-H}{\alpha_H}\right)\right) - \alpha_M\left(exp\left(\frac{-tp}{\alpha_R}\right) - exp\left(\frac{-H}{\alpha_R}\right)\right)\right] \quad (2)$$

$$AGWP_3 = Ra\alpha_R^2\alpha_H C\left[1 - exp\left(\frac{-tp}{\alpha_R}\right) - \left(\frac{\alpha_H}{\alpha_H - \alpha_R}\right)\left(exp\left(\frac{-tp}{\alpha_H}\right) - exp\left(\frac{-tp}{\alpha_R}\right)\right)\right]\left[exp\left(\frac{-tp}{\alpha_R}\right) - exp\left(\frac{-H}{\alpha_R}\right)\right] \quad (3)$$

$$GWP_{H_2} = \frac{AGWP_{H_2}}{AGWP_{CO_2}} \quad (4)$$

According to equation (4), the AGWP for CO_2 over a 100-year time horizon is determined to be 8.95×10^{-14}. For hydrogen (H_2), the AGWP is calculated by summing AGWP1, AGWP2, and AGWP3. Additional details regarding the Global Warming Potential (GWP) can be found in

the Appendix A.

3.4. Environmental analysis

This study evaluates multiple environmental parameters, including fuel consumption, nitrogen oxides emissions, carbon dioxide emissions, and water vapor emissions. The fuel consumption and emissions modeling approach is adapted from the methodology of Dray et al. [15] utilizing a fuel burn rate-based model to estimate fuel use for both kerosene-powered and hydrogen-powered aircraft. Therefore, for an aircraft of type t, class s, and flight phase m, the fuel use is modeled as:

$$fuel_{tsm} = \eta_{tsm,0} + \eta_{tsm,1}D + \eta_{tsm,2}D.PL + \eta_{tsm,3}D^2 + \eta_{tsm,4}PL + \eta_{tsm,5}D^2.PL \quad (5)$$

Where, the D is ground distance flown, PL is the total aircraft payload including passengers and their freight, and the parameter η_{tsm} are estimated for different class of aircraft. This model is applicable for climb, cruise, and descent phases and their related η_{tsm} for kerosene aircraft are derived from PIANO-X performance model [27]. For other flight phases, the fuel consumption and emissions values are calculated based on standard fuel usage rates and emission factors specific to the aircraft type. For hydrogen-powered aircraft, empirical fuel consumption data for various flight phases remains limited, making direct comparisons with kerosene-powered aircraft challenging. Due to this uncertainty, this study scales the fuel consumption of hydrogen aircraft from their kerosene counterparts, following the methodology used in Aviation Integrated Model (AIM2015). This approach allows for a realistic estimation of fuel burn across takeoff, climb, cruise, descent, and landing, compensating for the lack of available real-world data on hydrogen-fueled aviation performance. A similar approach is applied to NO_x emissions modeling, using the following equation for the climb, cruise, and descent phases:

$$NO_{x\,tsm} = \vartheta_{tsm,0} + \vartheta_{tsm,1}D + \vartheta_{tsm,2}D.PL + \vartheta_{tsm,3}D^2 + \vartheta_{tsm,4}PL + \vartheta_{tsm,5}D^2.PL \quad (6)$$

The values of ϑ_{tsm} are derived from the results of performance modeling analyses. The quantities of CO_2 and H_2O emissions are derived directly from the fuel consumption values in each flight phase. For a detailed breakdown of the fuel consumption and emissions data for both kerosene-based and hydrogen-powered aircraft, refer to Appendix B.

3.5. Economic analysis

DOC are closely tied to the aircraft class, encompassing expenses such as fuel, maintenance, crew salaries, fees, and capital costs. These costs constitute the largest portion of overall operating expenses. Equation (3) can be utilized to calculate the DOC [19]:

$$DOC_{tot} = DOC_{cap} + DOC_{Maint} + DOC_{Crew} + DOC_{fees} + DOC_{Energy} \quad (7)$$

DOC_{cap} is formulated as below [28]:

$$DOC_{cap} = DOC_{Depreciation} + DOC_{Interest} + DOC_{Insurance} \quad (8)$$

$$DOC_{Depreciation} = \frac{C_{Aircraft}}{DP}(1 - RV) \quad (9)$$

$$DOC_{Interest} = R_a.ADP \quad (10)$$

$$DOC_{Insurance} = R_i.C_{Aircraft} \quad (11)$$

Where $C_{Aircraft}$ represents the cost of the aircraft, RV is the residual value, DP is the depreciation rate, R_a and R_i are the interest rate and insurance rate, respectively. To calculate the direct operating cost component related to interest, the Aircraft Delivery Price (ADP) is utilized, which is formulated as:

$$ADP = (1 + R_{s-a})C_{Airframe} + (1 + R_{s-e})C_{Engine} \quad (12)$$

In equation (8), R_{s-e} and R_{s-a} represent the rates associated with engine and airframe spares, respectively. It is important to note that the cost of producing the airframe ($C_{Airframe}$) has been calculated using the data from [29]. However, the cost of the aircraft engine (C_{Engine}) has been determined based on a different approach. We have employed a relationship that takes into account the hydrogen-powered complexity factor ($k_{LH2Engine}$), which accounts for the complexities associated with the production of hydrogen engines. In this case, the hydrogen-powered complexity factor has been set to 0.1 to reflect the additional considerations involved in manufacturing hydrogen engines [30].

$$C_{Engine} = 121.5\frac{\text{CEPCI}_{2024}}{\text{CEPCI}_{base.year}}\left(1 + k_{LH2Engine}\right)\left(Th_{sealevel}\right)^{1.00161} \quad (13)$$

The thrust (Th) is measured in pounds (lbs), and the Chemical Engineering Plant Cost Index (CEPCI) is employed to update the cost of the engine. This factor was incorporated into the airframe cost calculation. The operating costs related to airframe and engine maintenance are divided into two components: labor and material costs. The equations pertaining to these maintenance operational costs are as follows [31]:

$$DOC_{Maint} = DOC_{Airframe_{Material}} + DOC_{Airframe_{Labour}} + DOC_{Engine_{Material}} + DOC_{Engine_{Labour}} + DOC_{Burden} \quad (14)$$

$$DOC_{Airframe_{Material}} = \frac{C_{FHa}T_{flight} + C_{FCa}}{T_{block}}C_{FHa} = 3.08\frac{C_{Airframe}}{10^6}C_{FCa} = 6.24\frac{C_{Airframe}}{10^6} \quad (15)$$

$$DOC_{Airframe_{Labour}} = \frac{(K_{FHa}T_{flight} + K_{FCa})LR\sqrt{Mach}}{T_{block}} \quad (16)$$

$$K_{FHa} = 0.59K_{FCa}K_{FCa} = 0.05\frac{W_{Airframe}}{1000} + 6 - \frac{630}{\frac{W_{Airframe}}{1000} + 120}$$

$$DOC_{Engine_{Material}} = \frac{C_{FHe}T_{flight} + C_{FCe}}{T_{block}} \quad (17)$$

$$C_{FHe} = 2.0n_e\frac{C_{Engine}}{10^5}C_{FCa} = 2.5n_e\frac{C_{Engine}}{10^5}$$

$$DOC_{Engine_{Labour}} = \frac{(K_{FHe}T_{flight} + K_{FCe})LR}{T_{block}} \quad (18)$$

$$K_{FHe} = (0.6 + 0.027\frac{Th_e}{1000})n_eK_{FCe} = (0.3 + 0.03\frac{Th_e}{1000})n_e$$

$$DOC_{Burden} = DOC_{Airframe_{Labour}} + DOC_{Engine_{Labour}} \quad (19)$$

Where T_{flight} and T_{block} (in hour) represent the flight time and block time, respectively. Block time officially commences when the aircraft begins moving from its parking position and concludes when it reaches a designated parking spot with all engines stopped. These two parameters are expressed in hours within the equations. LR denotes the labor rate in monetary units ($), while $W_{Airframe}$ represents the airframe weight. Th_e and n_e correspond to the engine thrust and the number of engines, respectively. It is noteworthy that the airframe weight is measured in kilograms (kg), while the engine thrust is expressed in pounds-force (lbf). The weight of conventional aircraft is calculated using the model presented in [32]. For hydrogen-powered aircraft, modifications are made to account for the weight of the hydrogen tank and the associated thermal management equipment. These additions are incorporated into the overall weight of the hydrogen aircraft using a gravimetric efficiency. Conversely, the weight reduction resulting from a decrease in the number of passenger seats, necessitated by the accommodation of the hydrogen tank, is also factored into the overall weight calculation for

hydrogen-powered aircraft. Equation (16) is employed to calculate the operating costs associated with the flight crew. There exists a divergence of opinion regarding whether crew operating costs should be categorized as direct or indirect operating costs. However, since crew costs vary based on the aircraft type, it is logical to consider these costs within the scope of direct operating costs [28].

$$DOC_{Crew} = DOC_{Cockpit} + DOC_{Attendant} \tag{20}$$

$$DOC_{Cockpit} = n_{pilot} LR_{pilot} \tag{21}$$

$$DOC_{Crew} = n_{att} LR_{att} \tag{22}$$

In equations (16) and (17), 'n' represents the number of pilots and flight attendants. To calculate the number of pilots, we refer to the flight time. For flight times exceeding 8 h, 3 pilots are considered, while for flights under 8 h, 2 pilots are considered. Regarding flight attendants, it is assumed that one flight attendant is required for every 30 passengers. The DOC associated with fees are segregated into distinct components. In the present study, the following items are accounted for as DOC pertaining to fees:

$$DOC_{fees} = DOC_{handling} + DOC_{landing} + DOC_{ATC} + DOC_{parking} + DOC_{CO_2} + DOC_{NO_x} \tag{23}$$

$$DOC_{handling} = p_{handling}.PL \tag{24}$$

$$DOC_{ATC} = f_{ATC}.Range.\sqrt{\frac{MTOW}{50000}} \tag{25}$$

$$DOC_{parking} = Constant.(based\ on\ aircraft\ size\ classes) \tag{26}$$

$$DOC_{CO_2} = p_{CO_2}.W_{emittedCO_2} \tag{27}$$

$$DOC_{NO_x} = p_{NO_x}.W_{emittedNO_x} \tag{28}$$

Regarding the direct operating costs pertaining to fees, the range dimension is expressed in kilometers (km), and all weight measurements are based on kilograms (kg). It is noteworthy that the abbreviation "ATC" stands for air traffic control. The DOC of fees also encompasses the costs associated with CO_2 and NO_x emissions. These emission costs are computed based on the quantities of CO_2 and NO_x released along the aircraft's flight. The present study delves into the DOC stemming from energy consumption, taking into account two distinct fuel types: hydrogen and JetA. The following equation outlines the relationship governing the DOC associated with energy [19]:

$$DOC_{energy} = p_{fuel}.W_{Blockfuel} \tag{29}$$

It is noteworthy that the formulation of the DOC of energy takes into account the weight of fuel consumed across all flight phases, commonly referred to as block fuel, which is measured in kilograms. This weight is then coupled with the production cost per kilogram of fuel, forming the fundamental basis of the equation that governs the DOC associated with energy consumption.

3.6. Hydrogen storage

Under ambient pressure and temperature, hydrogen has a very low volumetric energy density [33], making it impractical for direct use as aviation fuel. To address this challenge, hydrogen must be stored in either compressed gas or liquid form. When utilizing liquid hydrogen (LH_2), it must be maintained at temperatures below 20 K [34,35], necessitating a thermal management system to prevent boil-off losses. In this study, the hydrogen storage tanks are designed assuming a dual-tank configuration to maintain aircraft balance. One tank holds 40 % of the fuel and is positioned at the front of the fuselage, while the remaining 60 % is stored in a rear-mounted tank [36]. Fig. 2 illustrates the proposed tank integration within the fuselage. To estimate the additional weight introduced by hydrogen storage tanks, the gravimetric efficiency is calculated using the following equation [14]:

$$\gamma_{tank} = \frac{W_{H_2}}{W_{H_2} + W_{tank}} \tag{30}$$

where W_{H_2} represents the weight of the stored hydrogen fuel, and W_{tank} refers to the weight of the empty storage tank. Additionally, fuel weight calculations consider not only the amount required for the flight but also reserve fuel for route deviations and alternate airport landings.

3.7. Performance criteria

To evaluate the climate impact of Jet-A and hydrogen-powered aircraft, this study utilizes CO_2-equivalent emissions calculations, incorporating various greenhouse gases. The emissions for both propulsion systems are estimated using the following formulas:

$$W_{CO_2eq_{direct}} = W_{CO_2} + W_{NO_x} GWP_{NO_{x100}} + W_{H_2O} GWP_{H_2O_{100}} \tag{31}$$

$$W_{CO_2eq_{direct}} = W_{NO_x} GWP_{NO_{x100}} + W_{H_2O} GWP_{H_2O_{100}} + W_{H_2} GWP_{H_{2100}} \tag{32}$$

where GWP100 represents the global warming potential over a 100-year time horizon, and W_{H_2} denotes the amount of unburned or leaked hydrogen into the atmosphere.

Total emissions include both direct aircraft emissions and emissions from energy production pathways. To provide a standardized measure across aircraft types, total emissions per 100 Available Seat Kilometers (100ASK) are determined using the following equation:

$$W_{CO_2eq_{tot}} = 100 * \frac{(W_{CO_2eq_{direct}} + W_{CO_2eq_{pathway}})}{seat.distance} \tag{33}$$

As retrofitting aircraft to use hydrogen fuel typically reduces the number of available seats due to space requirements for hydrogen storage tanks, this factor is accounted for in emission calculations. Additionally, emissions from fuel transportation to airports are excluded from $W_{CO_2eq_{pathway}}$ computations.

From an economic perspective, total costs are determined by aggregating individual cost components. The economic impact is then normalized by considering the available seats and distance traveled:

Fig. 2. The structure of a non-integral tank carries hydrogen fuel used in the present study. The design of the hydrogen storage tank includes a hatch to ensure access to all regions of the aircraft.

$$DOC_{tot} = 100^{*}\frac{\sum DOC_k}{seat.distance} \tag{34}$$

To assess the environmental penalty associated with different hydrogen production pathways, a penalty factor (P_i) is introduced, measured in kg CO_2-equivalent per kg of fuel. This metric allows for a comparative evaluation of the climate impact of various hydrogen production methods relative to conventional kerosene-based aviation fuel:

$$P_i = \frac{CO_2eq_{H_2,leakage} + CO_2eq_{H_2,production} - CO_2eq_{Jet_A,production}}{W_{H_2}} \tag{35}$$

Since fossil fuels are not used in the selected hydrogen production pathways, the W_{Jet_A} value is set to zero in this study. To effectively evaluate the trade-offs between cost and emissions across different aircraft classes and hydrogen production pathways, two indices are introduced:

1. Cost per unit of emission reduction (CUPER): Measures the additional cost incurred per unit of CO_2-equivalent reduction compared to Jet-A

$$CUPER = \frac{DOC_{tot,H_2} - DOC_{tot,JetA}}{W_{CO_2eq_{tot,JetA}} - W_{CO_2eq_{tot,H_2}}}, \tag{36}$$

2. Eco-Efficiency Index (EEI): Provides a comprehensive measure by integrating cost and emission impacts into a single value, where both factors are normalized against a reference and weighted equally

$$EEI = \omega_{cost}\frac{DOC_{tot,H_2}}{DOC_{tot,JetA}} + \omega_{emission}\frac{W_{CO_2eq_{tot,H_2}}}{W_{CO_2eq_{tot,JetA}}}, \tag{37}$$

where, the ω_{cost} and $\omega_{emission}$ are the weighting factors that sum to 1. Since cost and emissions are equally important in this study, we assign both factors a value of 0.5.

3.8. Basic input and limitation of the study

To make a rational comparison in this study, we utilize real data from different regions, which was extracted from the AIM2015 database by analyzing scheduled flights. Table 2 illustrates the payload of both aircraft classes across different regions, while Table 3 presents the average distance flown by different aircraft classes across various regions, as utilized in this study. After computing the values for each region, their average is reported as a global metric in the results section.

Despite our efforts to conduct a comprehensive analysis, this study has inherent limitations that must be acknowledged. Several factors may influence the scope and accuracy of our findings. The key limitations are detailed below:

- The analysis does not account for potential leakage of pure hydrogen during the production process.
- Emissions resulting from transferring hydrogen from production facilities to airport storage tanks are not considered, under the assumption that production sites are situated near airports.
- The performance metrics for hydrogen-powered aircraft are derived solely by comparing the energy density ratios of kerosene and hydrogen, which may oversimplify real-world performance differences based on [12,37].
- The study does not include sensitivity analyses for the various hydrogen production pathways, which could provide insight into the robustness of the results under different scenarios.
- In calculating the life cycle emissions of kerosene, we assume a carbon intensity of 0.6 kg CO_2-equivalent per kg of kerosene. This figure encompasses emissions from crude oil extraction, transportation, and refining processes [38].

3.9. Economic and environmental modelling process

This study focuses on evaluating the performance of retrofitted hydrogen-powered aircraft by developing a computational model divided into six specialized modules. Each module addresses a distinct aspect of the analysis, ensuring a comprehensive assessment of hydrogen integration into aviation. The first module, the Aircraft Weight Estimator, determines the airframe weight based on key parameters, including structural design and aircraft dimensions. This estimation accounts for modifications required to incorporate hydrogen fuel systems. The second module, the Aircraft Cost Calculator, evaluates expenses related to adapting the aircraft for hydrogen usage, including modifications to the fuel tanks, delivery systems, and necessary structural reinforcements. The Seat Configuration Module plays a crucial role in adjusting the cabin layout to accommodate hydrogen storage. The Weight Adjustment Module estimates changes in payload, operational weight, and takeoff weight, incorporating the added mass of hydrogen fuel systems and the resulting impact on weight distribution. Among the most significant components of the model are the Aircraft Performance Module and the direct operating cost Module. The Aircraft Performance Module simulates key operational parameters, such as fuel consumption, emissions, and flight duration, by factoring in aircraft class, payload, and engine efficiency. Meanwhile, the DOC Module provides a financial assessment by calculating expenses related to capital investment, fuel, maintenance, crew wages, and airport fees, offering insights into the economic feasibility of hydrogen propulsion. In addition to these core modules, the study integrates various data sets to enhance calculation accuracy. Fig. 3 presents a simplified flowchart, illustrating the structure and interaction between modules, as well as the primary inputs and outputs within the computational framework. This visualization provides a clear representation of the model's functional design and interdependencies.

4. Model validation

Fig. 4 compares block fuel usage between the present study and the AIM2015 code [15] for small, medium, large twin aisle, and very large aircraft, representing long-range flights across various distance ranges. The x-axis represents the distance in kilometers (3,000–10,000 km), while the y-axis shows the block fuel usage in kilograms. Each subplot within Fig. 4 displays the block fuel consumption trends for a specific aircraft size class. The blue line represents the results of the current study, while the purple dots correspond to the outcomes from the AIM2015 code. As shown in Fig. 4, for four aircraft size classes, block fuel consumption increases with distance, following an approximately linear trend. This behavior is expected, as longer flights require more fuel. Notably, the present study and AIM2015 code yield comparable

Table 2
Aircraft payload (kg) by class and region based on data from the AIM2015 for scheduled flights.

Aircraft class	North America	Central America	South America	Europe	Middle East	Africa	Asia Pacific
Small twin-aisle	24,748	22,551	24,284	25,389	21,817	20,265	22,666
Medium twin-aisle	26,039	23,763	25,657	27,029	23,385	21,973	23,911
Large twin-aisle	33,058	28,350	32,090	34,778	28,826	28,510	30,527
Very large aircraft	42,941	37,285	42,833	45,268	38,308	40,318	42,143

Table 3
Aircraft traveled distance (km) by class and region based on data from the AIM2015 for scheduled flights.

Aircraft class	North America	Central America	South America	Europe	Middle East	Africa	Asia Pacific
Small twin-aisle	6786	6328	6895	6738	3707	5495	4529
Medium twin-aisle	6652	6005	5488	6664	4289	5188	2606
Large twin-aisle	8855	6087	8202	7618	5201	6474	4087
Very large aircraft	9192	4188	9091	7934	3495	9001	6827

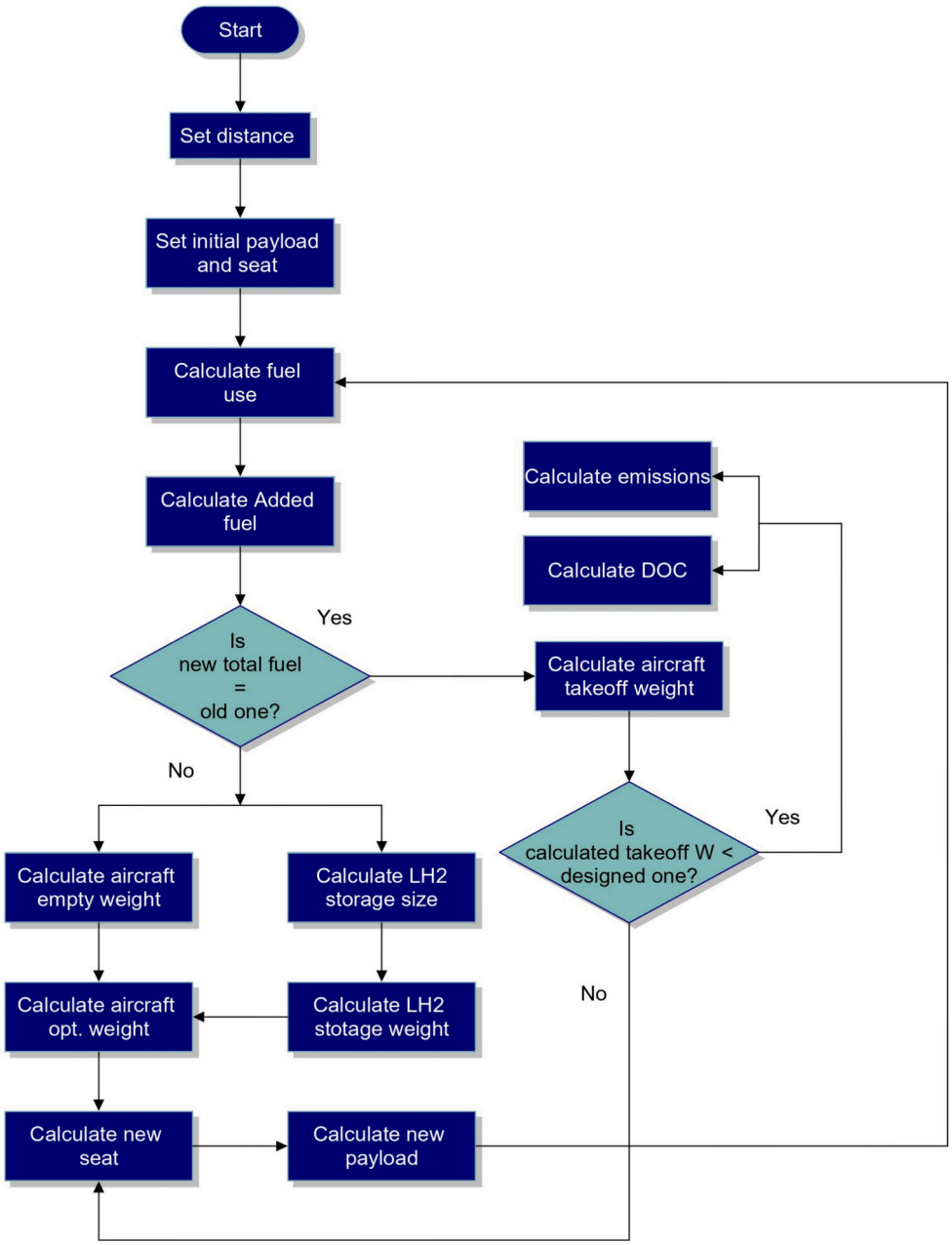

Fig. 3. Simplified flowchart of the present study, illustrating the interconnectivity between the six main modules: Aircraft Weight Calculator, Aircraft Cost Estimator, Seat Adjustment Module, Weight Estimator, Aircraft Performance Module, and Aircraft DOC Module.

trends and values across different aircraft sizes and distance ranges. This alignment indicates that this study produces fuel consumption estimates consistent with AIM2015. However, minor discrepancies exist between the four datasets, likely due to variations in the input parameters used in each study.

Fig. 5 illustrates the comparison of NO_x emissions between the present study and the AIM2015 code for four aircraft size classes across different flight distances. In each subplot, the red dots represent the NO_x emissions calculated by the AIM2015 code, and the brown line represents the NO_x emissions calculated by the present study. It is important to highlight that all inputs used for NO_x calculations in this section are based on existing reference data for the average NO_x emissions of fossil-fueled aircraft. The figure illustrates a clear upward trend in NO_x emissions as flight distance increases across both studies and for four

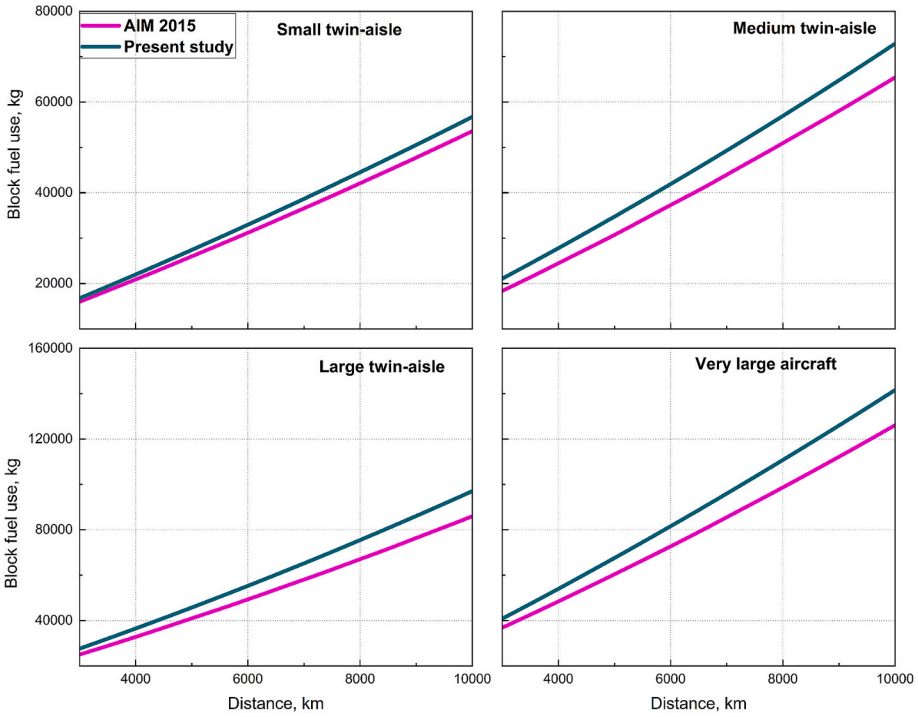

Fig. 4. Model verification in terms of block fuel use for the four-reference aircraft with AIM2015. The payload is set to be 100 kg.

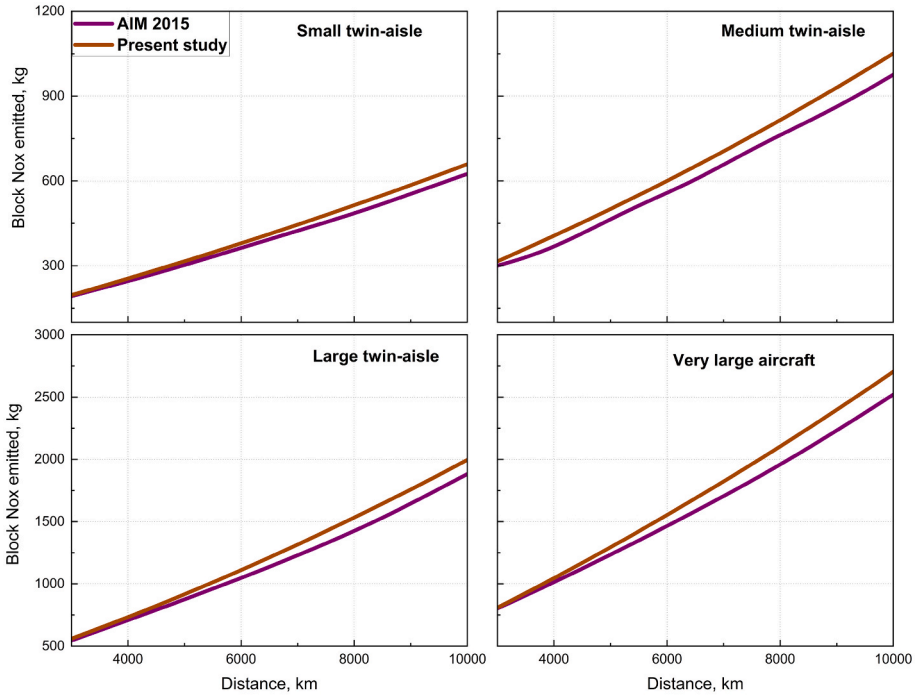

Fig. 5. Model verification in terms of NO_x emitted for the four-reference aircraft with AIM2015. The payload is set to be 100 kg.

aircraft size classes. When comparing results, it is evident that the present study generally predicts higher NO_x emissions than the AIM2015 code for very large aircraft. This difference likely stems from variations in the input parameters used in each model. Despite this discrepancy, the overall trends remain consistent, with both studies displaying a steady increase in NO_x emissions as flight distance extends. By visually examining the relationship between block fuel consumption and NO_x emissions from both models, the figure serves as a validation measure, confirming that the current study's model produces results that align with established computational methodologies, such as the AIM2015 code [15].

5. Results and discussion

This section is structured into six subsections: “jet-A and LH2 fuel use ”, “ CO_2-equivalent emissions of jet-A and LH_2-powered aircraft”, “ Direct operating costs of Jet-A and LH_2-powered aircraft”, “ Sensitive analysis on NO_x emission”, “Trade-offs between cost and emissions”, and “ Penalty for adopting hydrogen pathways.” Each topic is explored in detail in the following subsection.

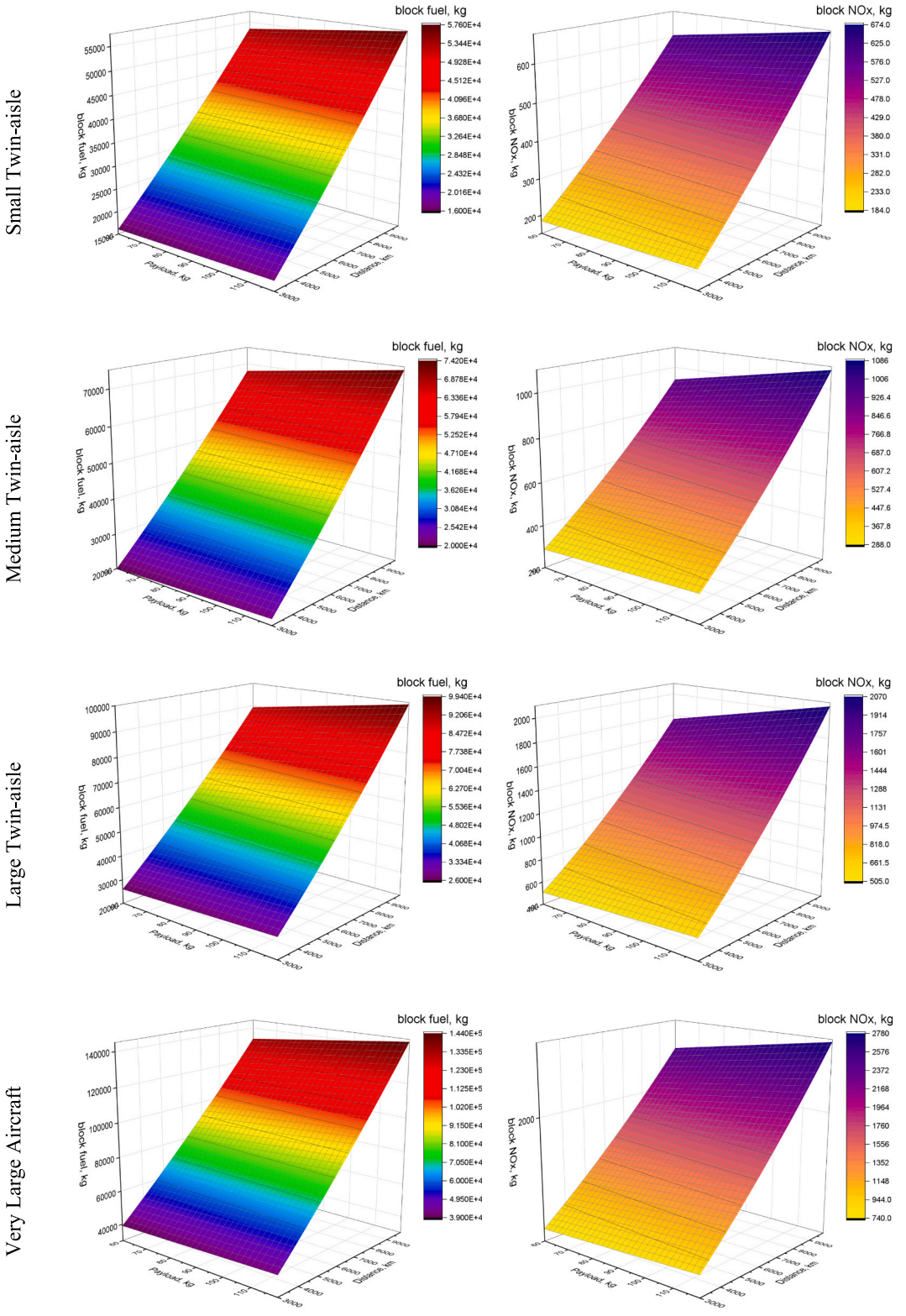

Fig. 6. Three-dimensional visualization of block fuel (JetA) consumption (left panels) and NO_x emissions (right panels) across varying flight distances (3,000–10,000 km) and payload ranges (60–120 kg) for small twin-aisle, medium twin-aisle, large twin-aisle, and very large aircraft classes. The color gradients indicate the magnitude of fuel use and NO_x emissions, clearly illustrating the relationship and trends with increasing distance and payload.

5.1. Jet-A and LH_2 fuel use

Fig. 6 provides a comprehensive visualization of how variations in payload (ranging from 60 to 120 kg) and flight distance (3,000–10,000 km) influence the block fuel (JetA) consumption and NO_x emissions for four different aircraft size classes (small twin-aisle, medium twin-aisle, large twin-aisle, and very large aircraft). The results exhibit clear and intuitive trends, demonstrating significant increases in both fuel usage and NO_x emissions as either payload or distance increases. Specifically, fuel consumption exhibits a pronounced sensitivity to changes in flight distance, indicated by a steeper gradient along the distance axis, while payload variations produce a slightly less pronounced, yet still considerable effect. As expected, larger aircraft categories exhibit substantially higher absolute fuel consumption and NO_x emissions compared to smaller aircraft classes. Regarding NO_x emissions, similar trends are observed, clearly correlating increased payload and distance with higher emissions. The nonlinear behavior highlighted by the three-dimensional visualization emphasizes the compounded effects of simultaneous increases in payload and range.

Fig. 7 illustrates a comparative analysis of JetA and liquid hydrogen (LH_2) fuel consumption across various global regions, segmented by aircraft size classes, the payload and ground distance extracted from Table 2 and 3, respectively. The results clearly indicate that LH_2 consistently demonstrates significantly lower block fuel consumption (in kg) compared to JetA for all aircraft classes and regions analyzed. This notable reduction is attributed primarily to hydrogen's higher gravimetric energy density compared to traditional kerosene (JetA). For small twin-aisle aircraft, the LH_2/JetA ratio exhibits minor regional variations, ranging approximately from 0.379 to 0.39, with slightly more favorable efficiency in North America (0.38) and Europe (0.379). In the medium twin-aisle category, this ratio remains relatively consistent, typically between 0.38 and 0.39, with the lowest ratio (0.38) found in the Asia-Pacific region, indicating optimal hydrogen efficiency. The large twin-aisle aircraft show a stable LH_2/JetA ratio of around 0.39 across regions, with minor variations such as Central America (~0.39) and Africa (~0.40), clearly highlighting hydrogen's consistent mass efficiency. Similarly, for very large aircraft, the LH_2 usage consistently yields a ratio close to 0.40, with regions such as North America, Europe, and Africa presenting comparable efficiencies. These findings emphasize the substantial potential of LH_2 to reduce block fuel mass requirements across all aircraft sizes and operating regions, typically achieving mass savings of approximately 60–63 % compared to traditional JetA fuel.

5.2. CO_2-equivalent emissions of jet-A and LH_2-powered aircraft

Fig. 8 presents the CO_2-equivalent emissions of Jet-A and Hydroprocessed Esters and Fatty Acids(HEFA) produced from palm oil aircraft alongside retrofitted hydrogen-powered aircraft across four different long-range aircraft classes, considering six distinct hydrogen production pathways. The environmental parameters analyzed in this study include direct emissions of CO_2, NO_x, H_2O, and greenhouse gases (GHGs) associated with the fuel life cycle. It is worth noting that the lifecycle emissions of HEFA are evaluated based on the energy used, with total emissions estimated at approximately 90 g CO_2-eq/MJ [39], covering the entire lifecycle from extraction to combustion. A key innovation of this research is the inclusion of pure hydrogen emissions into the atmosphere in hydrogen-powered scenarios, a factor often overlooked in similar assessments. To enable a meaningful comparison, emissions for all aircraft classes are measured in kilograms per 100 Available Seat Kilometers (kg CO_2eq/100 ASK). Overall, Fig. 8 shows a clear distinction between Jet-A, HEFA, and hydrogen-based pathways across all four aircraft classes (small/medium/large twin-aisle and very large aircraft). Jet-A consistently exhibits direct CO_2 and NO_x emissions, but its fuel-life-cycle contribution is relatively modest. By contrast, hydrogen pathways incur zero direct CO_2 at the engine level; however, their life-cycle CO_2-equivalent emissions can be significantly higher, depending on the production route. Water vapor also rises in hydrogen scenarios, and there is an added factor of direct hydrogen release (pure H_2), which can have non-negligible climate impacts. For all four aircraft classes, the lifecycle emissions associated with sustainable aviation fuel (SAF) derived from palm oil are approximately equivalent to those of conventional kerosene (JetA), and both exhibit significantly lower

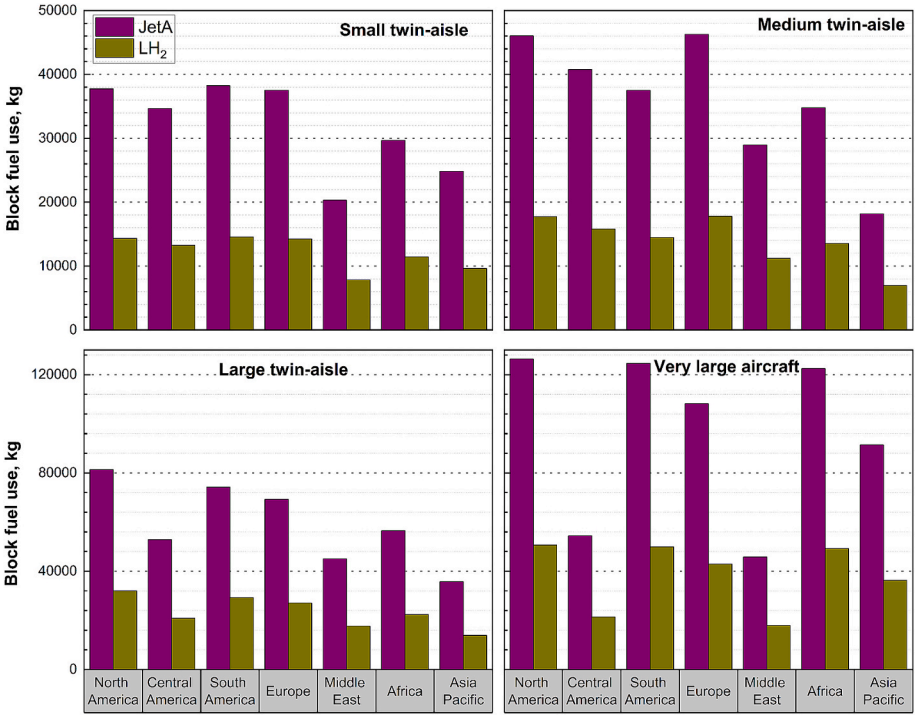

Fig. 7. Block fuel consumption comparison (in kg) between JetA and liquid hydrogen (LH_2) for different aircraft classes (small twin-aisle, medium twin-aisle, large twin-aisle, and very large aircraft) across various global regions.

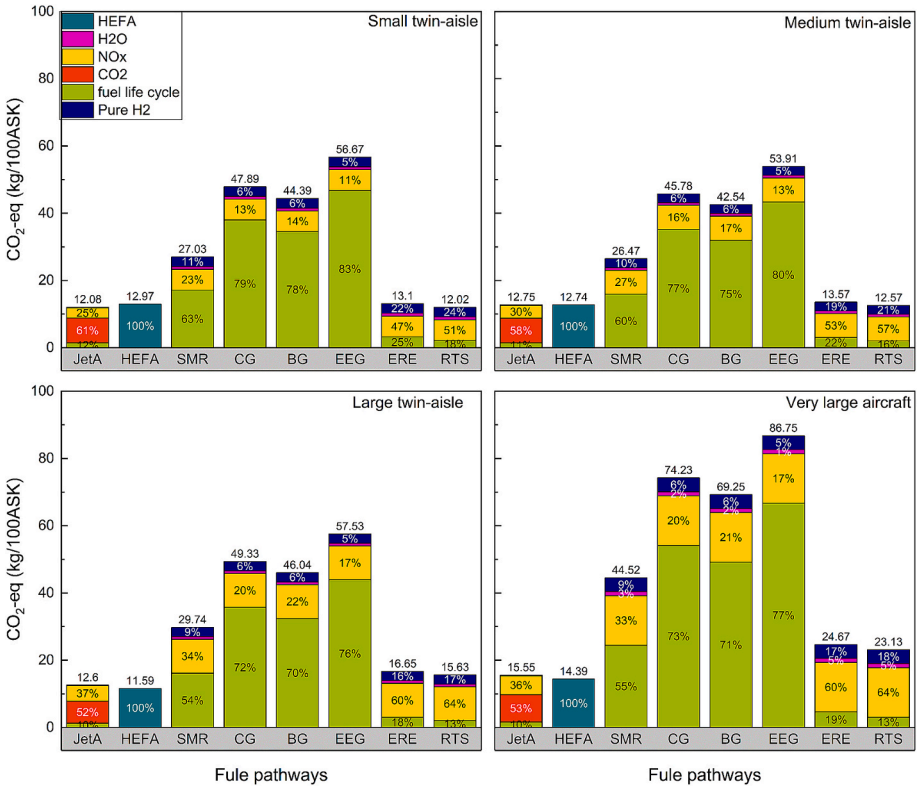

Fig. 8. Comparison of CO_2-equivalent emissions between HEFA, Jet-A, and hydrogen-powered aircraft across four long-range aircraft classes (small, medium, large twin-aisle, and very large). Six hydrogen production pathways are examined (SMR, CG, BG, EEG, ERE, and RTS), illustrating how their varying carbon footprints, NO_x outputs, and pure hydrogen releases influence total emissions.

emissions compared to hydrogen-based pathways. For small and medium twin-aisle aircraft, Jet-A emits direct CO_2 in the range of 7.3–7.4 kg/100 ASK and NO_x around 3–3.8 kg/100 ASK, with an additional 1–1.4 kg/100 ASK of fuel life-cycle CO_2-equivalent. For both small and medium twin-aisle aircraft, lifecycle emissions for HEFA are approximately 12.97 and 12.74 kg CO_2-eq/100 ASK, respectively, closely matching emissions from conventional JetA fuel. By contrast, hydrogen pathways substantially remove direct CO_2 at the engine level but still produce some NO_x. The total CO_2-equivalent for hydrogen-powered aircraft ranges from 12–13.6 kg/100 ASK (ERE, RTS) to 53.9–56.7 kg/100 ASK (EEG), driven primarily by the carbon footprint of hydrogen production. Emissions of pure hydrogen in these two aircraft classes are 2.6–2.9 kg CO_2eq/100 ASK, adding another dimension to the overall climate impact. The pattern persists but becomes more pronounced in large twin-aisle and very large aircraft. Jet-A emits 6.5–8.2 kg of direct CO_2 and 4.6–5.6 kg of NO_x per 100 ASK, along with 1–1.6 kg/100 ASK of life-cycle CO_2-equivalent, while the HEFA emits 11.59 and 14.39 kg CO_2-eq/100ASK. Hydrogen-driven propulsion again remove direct CO_2 but can exhibit higher NO_x. Depending on the production pathway, its life-cycle CO_2-equivalent ranges from about 15–24 kg/100 ASK (ERE, RTS) to as high as 86 kg/100 ASK (EEG). Moreover, larger aircraft produce greater water vapor and release more pure hydrogen, amplifying these non-CO_2 warming effects.

As shown in Fig. 8, across all aircraft classes, retrofitting aircraft to burn hydrogen instead of Jet A leads to higher CO_2-equivalent emissions. Two main factors contribute to this increase. First, the carbon footprint of hydrogen production—particularly in fossil-based or grid-dependent electrolysis pathways—adds to overall emissions. Second, there is an anticipated rise in NO_x output, stemming from limited and uncertain data on NO_x generation in hydrogen combustion systems. When comparing the ERE and EEG hydrogen production pathways to a Jet A baseline across various aircraft sizes, the ERE route shows a comparatively modest increase in total emissions—8% for small twin-aisle, 6.4 % for medium twin-aisle, 32 % for large twin-aisle, and 58 % for very large aircraft. Moreover, NO_x accounts for nearly 60 % of the overall emissions in ERE, reflecting the importance of NO_x mitigation strategies. In contrast, the EEG pathway exhibits dramatically higher emission increases, ranging from 370 % for small twin-aisle and 322 % for medium twin-aisle to 350 % for large twin-aisle and 457 % for very large aircraft. These findings highlight that, while ERE may remain viable with proper emissions controls, EEG's substantial emissions penalty makes it far less suitable as a sustainable alternative.

5.3. *Direct operating costs of Jet-A and LH_2-powered aircraft*

Fig. 9 presents the direct operating cost of Jet-A-powered aircraft alongside retrofitted hydrogen-powered aircraft across four different long-range aircraft classes, considering six distinct hydrogen production pathways. The cost parameters analyzed in this study include capital, maintenance, fess, crew, and cost associated with the fuel life cycle. To enable a meaningful comparison, emissions for all aircraft classes are measured in united states dollar ($) per 100 Available Seat Kilometers ($/100 ASK). Across all four aircraft classes, Jet-A consistently offers the lowest direct operating cost, ranging between 5.5 and 6.5 $/100 ASK overall. In contrast, hydrogen-powered aircraft—regardless of the production pathway—incur higher expenditures. Two primary drivers explain this difference. First, retrofitting aircraft to accommodate hydrogen increases both capital and maintenance costs, reflecting new system designs and the supporting infrastructure. Second, the energy component of DOC often rises, especially for production pathways heavily reliant on expensive feedstocks or electricity (e.g., EEG or CG). Among the hydrogen pathways, BG and SMR emerge as the most cost-effective, typically registering total costs 40–60 % above Jet-A. Other options like EEG, ERE, and CG push overall DOC even higher—often double or triple Jet-A costs—due to elevated energy prices, production complexities, and the need for extensive equipment upgrades. This cost

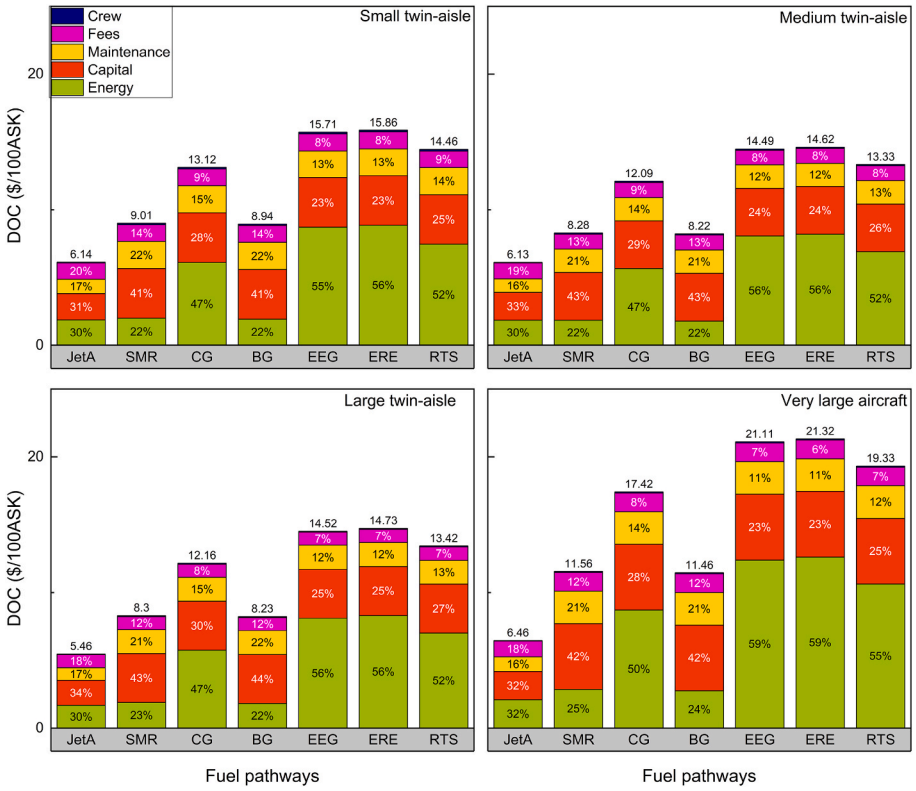

Fig. 9. Comparison of direct operating costs (DOC) for Jet-A and hydrogen-fueled aircraft across four long-range aircraft classes (small, medium, large twin-aisle, and very large). The chart highlights cost components—energy, capital, maintenance, fees, and crew—illustrating the higher overall costs for hydrogen propulsion, which vary with different production pathways.

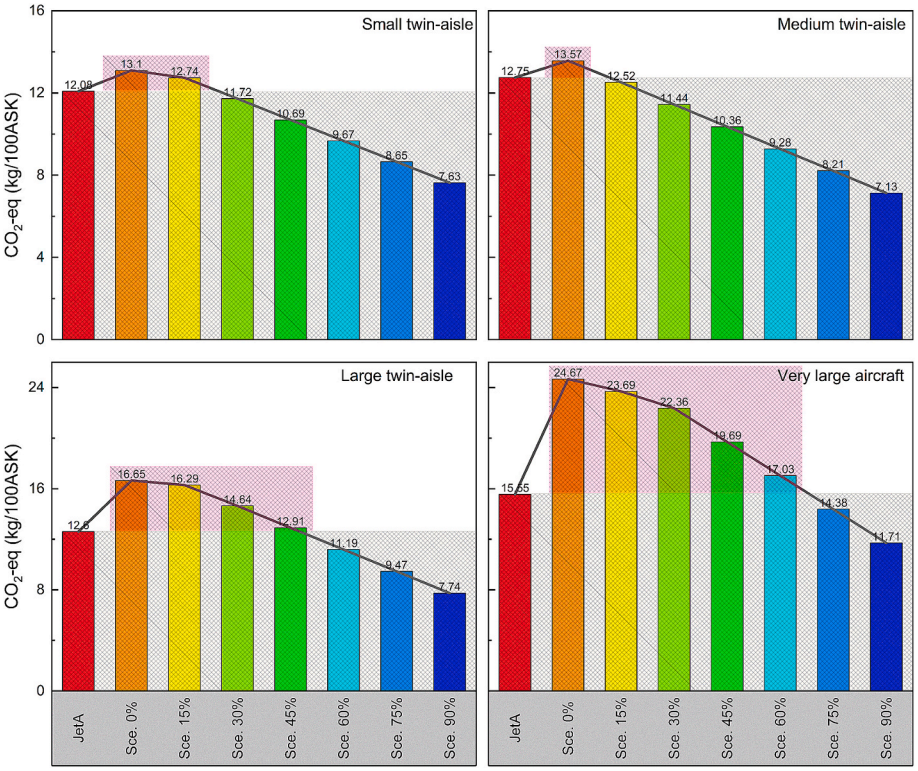

Fig. 10. Sensitivity analysis of NO_x reduction scenarios (15%, 30%, 45%, 60%, 75%, and 90%) for ERE-based hydrogen propulsion in four aircraft classes (small, medium, large twin-aisle, and very large). The results compare overall CO_2-equivalent emissions against a Jet A baseline, illustrating the thresholds at which ERE outperforms or converges with conventional kerosene.

premium becomes more pronounced for larger aircraft, where heightened fuel requirements amplify capital and energy expenditures. Consequently, while hydrogen retrofit pathways present potential environmental gains, their economic viability hinges on reducing hydrogen production costs and refining onboard systems to compete with Jet-A under commercial operating conditions.

5.4. Sensitive analysis

This section presents a detailed sensitivity analysis aimed at evaluating the robustness and reliability of our results under varying key assumptions and parameters. Specifically, we investigate how variations in NO_x emissions, well-to-tank (WTT) emissions associated with hydrogen production, and hydrogen production costs influence the environmental and economic outcomes of hydrogen-powered aviation.

5.4.1. Sensitive analysis on NOx emission

In the hydrogen-based aviation scenario, results indicate that fossil fuel-derived hydrogen production pathways and grid-based electrolysis offer no significant environmental advantages. Even renewable methods, such as renewable power-based electrolysis or renewable thermal splitting, provide only minimal benefits; for larger aircraft classes, these benefits can nearly disappear. Two main factors contribute to this outcome: the substantial emissions from certain hydrogen production pathways and the limited accuracy of current data on NO_x emissions at the engine level. While emissions from renewable hydrogen production are relatively minor compared to fossil-based pathways, the overall impact still depends heavily on precise NO_x estimates. To explore this aspect further, green hydrogen (electrolysis using renewable energy) is chosen as a possible route for a sensitivity analysis.

In this study, six reduction scenarios for NO_x—specifically 15 %, 30 %, 45 %, 60 %, 75 %, and 90 %—are evaluated to understand how diminishing NO_x emissions affect overall environmental outcomes. Fig. 10 illustrates the results of this sensitivity analysis in detail. The red hatches indicate the difference compared to the kerosene baseline. Under various NO_x reduction scenarios, the retrofitted hydrogen-powered aircraft still do not surpass kerosene in terms of overall carbon-equivalent emissions, showing no clear environmental advantage. Although hydrogen combustion initially incurs higher NO_x (and thus higher total CO_2-equivalent), reducing NO_x can bring ERE's emissions below the kerosene baseline—provided that the NO_x cut is substantial enough. In the small twin-aisle class, Jet A stands at 12.08 kg CO_2eq/100 ASK, whereas ERE without NO_x reduction (0 % scenario) climbs to 13.10 kg/100 ASK. Even at 15 % NO_x reduction, emissions remain slightly above Jet A, but from 30 % reduction onward (11.72 kg/100 ASK), ERE performs better. In the medium twin-aisle category, Jet A stands at 12.75 kg/100 ASK, while ERE with 0 % NO_x reduction produces 13.57 kg/100 ASK. Notably, at just 15 % NO_x reduction (resulting in 12.52 kg/100 ASK), the total emissions for ERE fall marginally below the Jet A baseline and continue to improve at higher reduction levels. For large twin-aisle aircraft, Jet A generates 12.60 kg/100 ASK, while ERE starts at 16.65 kg/100 ASK with 0 % NO_x reduction. Even a 45 % cut (yielding 12.91 kg/100 ASK) remains slightly higher than Jet A. Only at a 60 % reduction (11.19 kg/100 ASK) does ERE outperform Jet A. In the very large category, Jet A stands at 15.55 kg/100 ASK, whereas ERE begins at 24.67 kg/100 ASK (0 % scenario). A 60 % reduction (17.03 kg/100 ASK) is still higher than Jet A, but once the reduction reaches 75 % (14.38 kg/100 ASK), ERE's total CO_2-equivalent finally dips below the kerosene baseline.

5.4.2. Sensitive analysis on well-to-tank emission

To understand the influence of variations in well-to-tank (WTT) emissions of hydrogen production pathways on the overall emission profiles of hydrogen-powered aircraft, we performed a sensitivity analysis. This analysis considers six different WTT emission scenarios, ranging from very optimistic (1 and 2 kg CO_2eq per kg H_2) to highly conservative scenarios (10, 20, 25, and 30 kg CO_2eq per kg H_2). The sensitivity results for each aircraft size class are presented in Fig. 11. For small twin-aisle aircraft, JetA baseline emissions are 12.1 kg CO_2eq/100ASK. Hydrogen scenarios with very low WTT emissions (1–2 kg

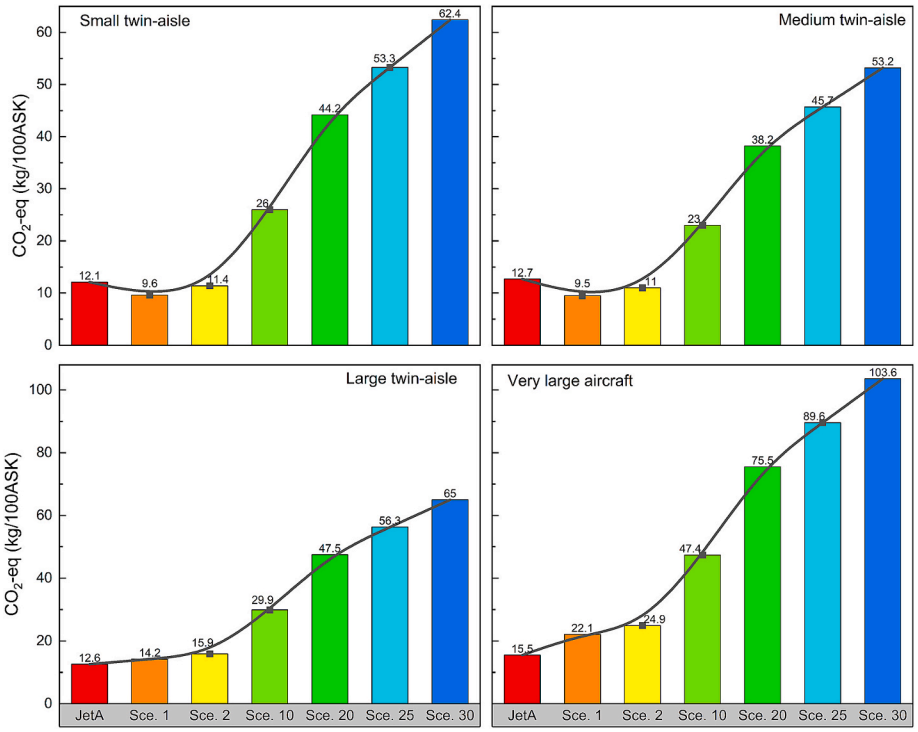

Fig. 11. Sensitivity analysis of total CO_2-equivalent emissions (kg CO_2eq/100 ASK) for JetA and liquid hydrogen (LH_2) under varying well-to-tank (WTT) emission scenarios (1–30 kg CO_2eq/kg H_2), shown for small, medium, large twin-aisle, and very large aircraft classes. The baseline JetA emissions are presented for comparison.

CO_2eq) show lower or comparable total emissions to JetA (9.6 and 11.4 kg CO_2eq respectively), indicating clear environmental benefits. However, at moderate to higher WTT emission scenarios (10 to 30 kg CO_2eq), total emissions rise sharply, surpassing JetA significantly. Specifically, scenario 10 increases emissions to 26 kg CO_2eq (+115 % over JetA), scenario 20 to 44.2 kg (+265 %), scenario 25 to 53.3 kg (+340 %), and scenario 30 to 62.4 kg (+415 %). For medium twin-aisle aircraft, the JetA baseline emissions are 12.7 kg CO_2eq/100ASK. Similar to small twin-aisle aircraft, hydrogen scenarios with low WTT emissions (scenarios 1 and 2) yield lower or similar emissions (9.5 and 11 kg CO_2eq). However, at higher emission scenarios (10, 20, 25, 30 kg CO_2eq), hydrogen emissions notably exceed the JetA baseline. Scenario 10 emissions rise to 23 kg CO_2eq (+81 %), scenario 20 reaches 38.2 kg (+201 %), scenario 25 is at 45.7 kg (+260 %), and scenario 30 peaks at 53.2 kg (+319 %). In the large twin-aisle aircraft, the JetA baseline is 12.6 kg CO_2eq/100ASK. For large aircraft, even optimistic hydrogen production scenarios (1–2 kg CO_2eq) result in slightly higher emissions than JetA (14.2 and 15.9 kg CO_2eq respectively), primarily due to larger fuel mass requirements. For more pessimistic scenarios, emissions increase substantially: scenario 10 to 29.9 kg (+137 %), scenario 20 to 47.5 kg (+277 %), scenario 25 to 56.3 kg (+347 %), and scenario 30 to 65 kg (+416 %). For very large aircraft, JetA emissions are higher (15.5 kg CO_2eq/100ASK) due to inherently larger fuel loads. For hydrogen scenarios, even optimistic scenarios significantly surpass the JetA baseline. Scenario 1 emissions reach 22.1 kg (+43 %), scenario 2 reaches 24.9 kg (+61 %), scenario 10 rises sharply to 47.4 kg (+206 %), scenario 20 further increases to 75.5 kg (+387 %), scenario 25 to 89.6 kg (+478 %), and scenario 30 culminates at 103.6 kg (+568 %). These results highlight a critical insight: the climate benefits of hydrogen-powered aviation are highly sensitive to the emissions intensity of hydrogen production. Only with low-emission hydrogen production methods (below approximately 2 kg CO_2eq per kg H_2) can clear environmental advantages be consistently realized compared to traditional JetA. Conversely, higher emission intensities during hydrogen production could significantly outweigh potential operational emission reductions, especially for larger aircraft classes.

5.4.3. Sensitive analysis on hydrogen production price

Fig. 12 presents a sensitivity analysis exploring the impact of hydrogen production cost variations (ranging from $1 to $5.5 per kg H_2) on the DOC for hydrogen-powered aircraft across different size classes. JetA serves as a baseline for comparison. The results indicate a clear and significant sensitivity of hydrogen aircraft operating costs to changes in hydrogen fuel price. At a low hydrogen price ($1/kg), DOC values already exceed JetA baseline values for all aircraft classes. As hydrogen prices increase from $1 to $5.5 per kg, DOC values rise considerably—by approximately 85 % for medium twin-aisle, 108 % for small twin-aisle, 88 % for large twin-aisle, and nearly 95 % for very large aircraft. These results underscore the critical importance of reducing hydrogen production costs to make hydrogen-powered aviation economically viable compared to conventional JetA-powered fleets.

5.5. Trade-offs between cost and emissions

Examining NO_x reduction scenarios alone may yield promising environmental benefits, but it is also crucial to compare the cost and emission trade-offs between fossil-fuel and hydrogen-powered aircraft across different classes. Such an evaluation requires considering both

Table 4
Eco-Efficiency Index (EEI) for ERE (electrolysis with renewable energy) across different aircraft classes (small twin-aisle, medium twin-aisle, large twin-aisle, and very large aircraft) under various NO_x reduction scenarios (0%–90%).

Scenario	Small twin-aisle	Medium twin-aisle	Large twin-aisle	Very large aircrfat
JetA	1	1	1	1
Sce. 0 %	1.84	1.73	2.3	2.47
Sce. 15 %	1.83	1.69	2.28	2.43
Sce. 30 %	1.78	1.64	2.21	2.39
Sce. 45 %	1.74	1.60	2.14	2.30
Sce. 60 %	1.70	1.55	2.07	2.21
Sce. 75 %	1.65	1.51	2.00	2.12
Sce. 90 %	1.61	1.47	1.93	2.03

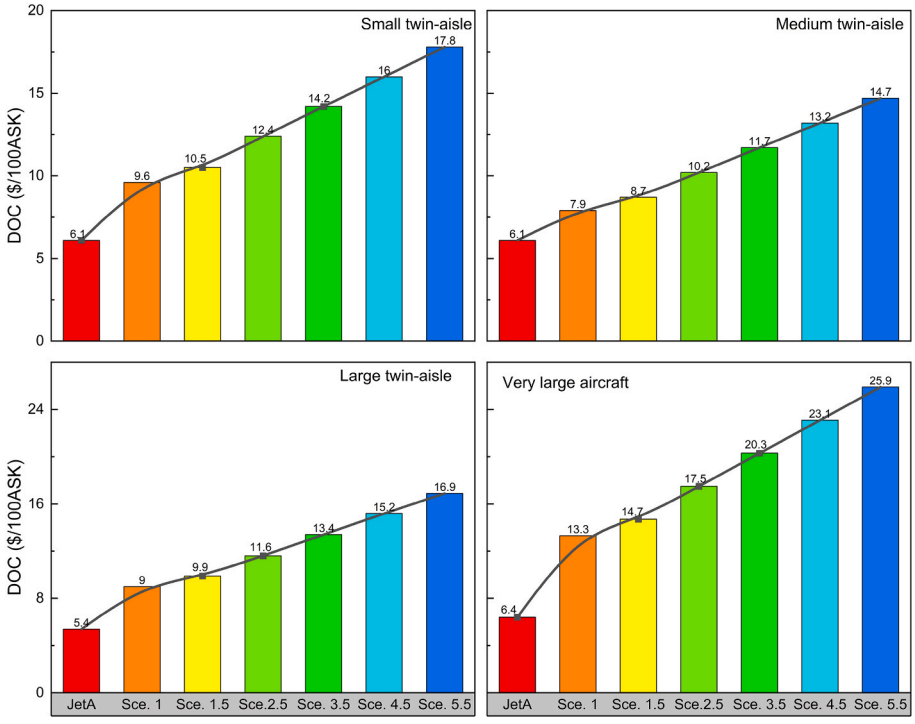

Fig. 12. Sensitivity analysis of total DOC ($/100 ASK) for JetA and liquid hydrogen (LH_2) under varying hydrogen production prices scenarios (1–5.5 $/kg H_2), shown for small, medium, large twin-aisle, and very large aircraft classes. The baseline JetA DOC are presented for comparison.

cost and emissions in tandem to achieve a comprehensive perspective on sustainable aviation.

Table 4 presents the Eco-Efficiency Index (EEI) results for the ERE pathway (electrolysis with renewable energy). It indicates that while hydrogen-powered aircraft offer potential environmental advantages, their overall eco-efficiency remains significantly higher than Jet A across all aircraft classes, even under progressive NO_x reduction scenarios. For small twin-aisle aircraft, the EEI starts at 1.84 in the 0 % reduction scenario and improves to 1.61 with a 90 % NO_x reduction, representing a modest gain in eco-efficiency. Similarly, in the medium twin-aisle category, the EEI begins at 1.73 and declines to 1.47 as NO_x reductions increase. These trends indicate that smaller aircraft in long-haul flights are relatively more responsive to NO_x reduction in improving their eco-efficiency, though they remain above the Jet A baseline (EEI = 1). In large twin-aisle aircraft, the EEI is higher, starting at 2.3 and improving only to 1.93 in the 90 % reduction scenario. For very large aircraft, the results are even more pronounced, with the EEI starting at 2.47 in the 0 % scenario and decreasing to 2.03 at 90 % reduction. These findings highlight that larger aircraft face greater challenges in achieving competitive eco-efficiency due to higher energy demands and the associated costs of hydrogen production and infrastructure.

Overall, the EEI analysis shows that while NO_x reduction improves eco-efficiency for all aircraft classes, retrofitted hydrogen-powered aircraft still struggle to compete with Jet A from a combined cost-emission perspective. Small and medium twin-aisle aircraft classes exhibit relatively better performance, making them more suitable for initial hydrogen adoption, while larger aircraft require further advancements in hydrogen production and NO_x mitigation to achieve competitive eco-efficiency.

Table 5 highlights the results of CUPER ($/$CO_2$eq) values for the ERE pathway. It reveals important insights into the cost-effectiveness of retrofitted hydrogen-powered aircraft under different NO_x reduction scenarios. The absence of CUPER values (indicated as "-") in certain scenarios implies that there is no net reduction in CO_2-equivalent emissions compared to Jet A, and thus, no cost-effectiveness can be assessed. In smaller aircraft classes (small and medium twin-aisle), hydrogen propulsion begins to show measurable CO_2-equivalent reductions from the 30 % NO_x reduction scenario, with CUPER improving from 27.25 $/$CO_2$eq to 2.19 $/$CO_2$eq at 90 % reduction. Medium twin-aisle aircraft exhibit better cost-effectiveness, starting at 37 $/$CO_2$eq (15)% NO_x reduction) and reaching 1.50 $/$CO_2$eq at 90 % reduction, indicating a more scalable transition. In contrast, for larger aircraft, no net CO_2-equivalent reductions are observed until 60 % NO_x reduction (CUPER: 8.75 $/$CO_2$eq for large twin-aisle, 12.79 $/$CO_2$eq for very large aircraft at 75 %). The required threshold for cost-effective CO_2-equivalent reduction increases with aircraft size, underscoring the operational and energy cost challenges of hydrogen adoption in larger configurations. These findings emphasize that while hydrogen-powered aviation can become economically viable, achieving this requires both high NO_x reduction and cost-efficient hydrogen production pathways to maximize the cost-emission trade-off.

Table 5
Cost per Unit of Emission Reduction (CUPER) values ($/$CO_2$eq) for ERE (electrolysis with renewable energy) across different aircraft classes (small twin-aisle, medium twin-aisle, large twin-aisle, and very large aircraft) under various NO_x reduction scenarios (15%–90%).

Scenario	Small twin-aisle	Medium twin-aisle	Large twin-aisle	Very large aircrfat
Sce. 0 %	–	–	–	–
Sce. 15 %	–	37	–	–
Sce. 30 %	27.25	6.49	–	–
Sce. 45 %	7.05	3.55	–	–
Sce. 60 %	4.06	2.44	8.75	–
Sce. 75 %	2.85	1.86	3.94	12.79
Sce. 90 %	2.19	1.50	2.53	3.89

5.6. Penalty for adopting hydrogen pathways

Fig. 13 illustrates the penalty factors (kg CO_2eq/kg fuel) associated with pure hydrogen leakage emissions across various hydrogen production pathways for long-range flights, while also comparing them to short-range aircraft. A lower penalty factor signifies a smaller additional environmental impact from hydrogen emissions relative to kerosene, indicating a more environmentally favorable production pathway. The penalty factor values provided represent the average across four long-range aircraft classes, showing little variation among them. This indicates that the environmental impact of hydrogen leakage remains relatively consistent across long-haul aircraft, regardless of specific size or configuration. Across fossil-based pathways and EEG, short-range aircraft exhibit higher penalty factors than long-range aircraft. The difference is most pronounced for fossil-based pathways, where the penalty for short-range aircraft is 20–25 % higher than for long-range aircraft. This may be due to higher hydrogen consumption rates in short-range operations, which amplifies the impact of leakage per unit of fuel used. Renewable hydrogen production pathways (ERE, RTS) emerge as the most environmentally favorable options, with penalty factors nearly an order of magnitude lower than those of fossil-based alternatives. Notably, while SMR, CG, BG, and EEG exhibit lower penalty factors for long-range aircraft compared to short-range aircraft, these pathways remain undesirable due to their high overall emissions. Conversely, ERE, which appears to be the most environmentally promising option, has a slightly higher penalty factor for long-range aircraft than for short-range aircraft, highlighting the complex trade-offs in hydrogen aviation sustainability.

6. Concluding remarks

The shift to hydrogen-powered aviation offers both promising opportunities and considerable challenges. This study provides a comprehensive evaluation of retrofitted long-range hydrogen aircraft, examining emissions, costs, and addressing the key question: Can improved long-range hydrogen aircraft ensure sustainable aviation? To explore this, the analysis considers six different hydrogen production pathways, evaluates scenarios for NO_x reduction at the engine level, and assesses the potential impact of pure hydrogen release into the atmosphere. The key findings of this study are summarized as follows:

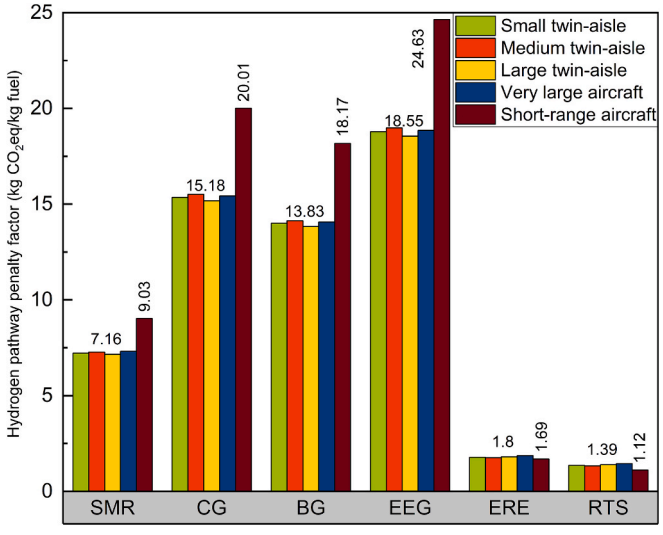

Fig. 13. Penalty factors (kg CO_2eq/kg fuel) associated with hydrogen leakage across different hydrogen production pathways for long-range and short-range aircraft.

- The findings reveal that, in a baseline scenario without NO_x mitigation, hydrogen-powered aircraft fail to achieve lower CO_2-equivalent emissions compared to kerosene-based aircraft. Even under low-emission hydrogen production pathways, such as renewable electrolysis (ERE), long-range hydrogen aircraft still produce 8.6 % to 58.6 % more emissions than their fossil-fuel counterparts.
- The direct operating cost (DOC) of hydrogen-powered aircraft using renewable electrolysis (ERE) is substantially higher than that of kerosene-powered aircraft across all four aircraft classes. The ERE pathway increases DOC by 91–132 % compared to Jet-A, with the cost impact being most significant in larger aircraft.
- The sensitivity analysis of NO_x emissions reduction reveals that substantial NO_x mitigation is required for hydrogen aircraft to achieve comparable or lower CO_2-equivalent emissions than kerosene-based aviation. While medium twin-aisle aircraft achieve parity at a 15 % NO_x reduction, larger aircraft require at least a 60–75 % NO_x reduction to become environmentally competitive.
- Sensitivity analyses indicate that hydrogen-powered aviation is environmentally advantageous over JetA only when well-to-tank (WTT) emissions remain below approximately 2 kg CO_2eq/kg H_2; beyond this threshold, hydrogen's climate benefits are significantly reduced or even reversed, especially for larger aircraft classes.
- Economic assessments highlight the critical importance of hydrogen production costs, showing substantial increases (85–108 %) in direct operating costs (DOC) as hydrogen prices rise from $1 to $5.5/kg H_2, emphasizing the necessity of cost reduction for hydrogen adoption in aviation.
- The EEI analysis highlights that even with progressive NO_x reduction, the overall eco-efficiency of hydrogen-powered aircraft remains lower than Jet-A across all aircraft classes.
- The CUPER values indicate that hydrogen aviation only becomes cost-effective at high NO_x reduction levels. Small and medium twin-aisle aircraft classes achieve competitive CUPER values at 30 % NO_x reduction, while larger aircraft require reductions of 60 % or more before cost-effectiveness is realized. These findings emphasize the necessity of both NO_x mitigation and cost reductions in hydrogen production for viable commercial deployment.
- The penalty factor for unburned hydrogen emissions underscores the environmental trade-offs of hydrogen aviation. Fossil-based hydrogen pathways and grid-powered electrolysis exhibit significantly higher penalties, while renewable hydrogen pathways (ERE, RTS) emerge as the most environmentally favorable options. However, in contrast to fossil-based pathways, where long-range aircraft have lower penalty factors than short-range aircraft, the opposite trend is observed for ERE.

CRediT authorship contribution statement

Saeed Rostami: Writing – review & editing, Writing – original draft, Visualization, Validation, Software, Methodology, Investigation, Data curation. **Khodayar Javadi:** Writing – review & editing, Supervision, Project administration, Investigation, Data curation. **Abbas Maleki:** Writing – review & editing, Supervision, Project administration, Investigation, Data curation.

Declaration of competing interest

The authors declare that they have no known competing financial interests or personal relationships that could have appeared to influence the work reported in this paper.

Acknowledgment

We sincerely appreciate Dr. Andreas W. Schäfer and Dr. Lynnette Dray from the UCL Energy Institute for their contribution in developing the AIM2015 code, which provided valuable support for our research. This study was conducted without any external funding.

Appendix A:. Data for calculating global warming potential for hydrogen

AGWP: Measured in watts per square meter per kilogram per year (W m^{-2} kg^{-1} yr^{-1}), AGWP quantifies the total radiative forcing impact of a greenhouse gas over a specific time horizon.

R (Radiative Forcing Scaling Factor): Represents the change in radiative forcing per unit concentration change, expressed in watts per square meter per part per billion (W m^{-2} ppb^{-1}) or for tropospheric ozone, in watts per square meter per Dobson unit (W m^{-2} DU^{-1}).

***a*:** The production rate of a species that results in indirect radiative forcing, measured as a change in mixing ratio per year (yr^{-1}) per ppb change in H_2 at steady-state.

α_R: The lifetime of the perturbation for the species causing radiative forcing.

α_H: The combined chemical and deposition lifetime of hydrogen (in years).

H: The time horizon considered for the AGWP calculation, which in this study includes 20 and 100 years.

C (Conversion Factor): Used to convert the hydrogen mixing ratio from parts per billion (ppb) to mass (kg).

tp (Length of Step Emission): The duration of the step emission, measured in years (yr).

Table A1
Basic inputs and parameters for the calculating AWGP of hydrogen [20].

	R	*a*	α_R	α_H	*C*
Stratospheric water vapour (at 30 km)	1e-4 W m^{-2} (ppb H_2O)$^{-1}$	0.042 ppb H_2O (ppb H_2)$^{-1}$ yr^{-1}	8 yr	1.9 yr	3.5e-9 ppb kg^{-1}
Tropospheric ozone	0.042 W m^{-2} DU^{-1}	0.0056 DU (ppb H_2)$^{-1}$ yr^{-1}	0.07 yr	1.9 yr	3.5e-9 ppb kg^{-1}

Table A2
GWP for the calculating CO_2eq.

	GWP 100	Ref.
H_2O	0.06	[40]
NO_x	114	[40]
H_2	10.8	Calculated

Appendix B:. Data for calculating fuel consumption and emissions of aircraft

.

Table B1
Basic inputs and parameters for the present study based on four reference aircraft class.

Size Category	Seat range	Ref. aircraft	Ref. engine	MTOW (kg)	Gravimetric efficiency	Aspect ratio	Wing area (ft2)
Small twin aisle	234	Boeing-787–800	Genx-1B67	227,900	0.55	11	3498
Medium twin aisle	293	Airbus-A330-300	Trent-772B	233,000	0.55	10.1	3908.4
Large twin aisle	427	Boeing-777-300ER	PW4090	351,530	0.55	9	4701.67
Very large aircraft	517	Airbus-A380-800	EA-GP7270	560,000	0.55	7.8	9096

Table B2
Basic inputs and parameters for the climbout flight phase for four reference aircraft[15].

Size Category		η_0	η_1	η_2	η_3	η_4	η_5	ϑ_0	ϑ_1	ϑ_2	ϑ_3	ϑ_4	ϑ_5
Small twin-aisle	JetA	2165.62	0.088751	−4.62E-07	−1.20E-07	0.020784	4.52E-11	35.92602	0.001308	2.94E-09	2.00E-08	0.000347	5.69E-13
	LH_2	777.4576	0.031861	−1.66E-07	−4.31E-08	0.007461	1.62E-11	35.92602	0.001308	2.94E-09	2.00E-08	0.000347	5.69E-13
Medium twin-aisle	JetA	2326.631	0.172577	−1.43E-06	−2.47E-06	0.028881	1.30E-10	62.47325	0.003662	−5.08E-10	2.32E-08	0.00072	2.11E-12
	LH_2	835.2606	0.061955	−5.13E-07	−8.87E-07	0.010368	4.67E-11	62.47325	0.003662	−5.08E-10	2.32E-08	0.00072	2.11E-12
Large twin-aisle	JetA	3266.149	0.055017	3.94E-07	2.83E-06	0.011822	4.80E-11	97.3941	0.002061	1.55E-08	1.06E-07	0.000442	1.60E-12
	LH_2	1172.548	0.019751	1.41E-07	1.02E-06	0.004244	1.72E-11	97.3941	0.002061	1.55E-08	1.06E-07	0.000442	1.60E-12
Very large aircraft	JetA	5226.88	0.315239	−1.66E-06	−1.08E-06	0.032369	1.79E-10	169.4941	0.007604	2.07E-08	2.40E-07	0.000942	2.46E-12
	LH_2	1876.45	0.113171	−5.96E-07	−3.88E-07	0.01162	6.43E-11	169.4941	0.007604	2.07E-08	2.40E-07	0.000942	2.46E-12

Table B3
Basic inputs and parameters for the cruise flight phase for four reference aircraft[15].

Size Category		η_0	η_1	η_2	η_3	η_4	η_5	ϑ_0	ϑ_1	ϑ_2	ϑ_3	ϑ_4	ϑ_5
Small twin-aisle	JetA	−1170.35	3.636845	2.71E-05	6.74E-05	−0.03229	9.72E-11	−6.55468	0.033711	4.41E-07	1.11E-06	−0.00054	1.99E-12
	LH_2	−420.157	1.305627	9.73E-06	2.42E-05	−0.01159	3.49E-11	−6.55468	0.033711	4.41E-07	1.11E-06	−0.00054	1.99E-12
Medium twin-aisle	JetA	−1446.86	4.391701	3.23E-05	9.51E-05	−0.03688	2.63E-10	−11.3725	0.043078	6.52E-07	1.97E-06	−0.0006	1.08E-11
	LH_2	−519.422	1.576621	1.16E-05	3.41E-05	−0.01324	9.44E-11	−11.3725	0.043078	6.52E-07	1.97E-06	−0.0006	1.08E-11
Large twin-aisle	JetA	−1882.57	5.621224	3.23E-05	0.000136	−0.01838	4.34E-10	−12.0511	0.078954	9.53E-07	4.18E-06	−0.00071	1.80E-11
	LH_2	−675.843	2.018019	1.16E-05	4.87E-05	−0.0066	1.56E-10	−12.0511	0.078954	9.53E-07	4.18E-06	−0.00071	1.80E-11
Very large aircraft	JetA	−3470.12	8.878538	3.31E-05	0.000182	−0.03803	−2.98E-11	−45.0001	0.12502	8.88E-07	4.94E-06	−0.00083	1.40E-12
	LH_2	−1245.77	3.187395	1.19E-05	6.55E-05	−0.01365	−1.07E-11	−45.0001	0.12502	8.88E-07	4.94E-06	−0.00083	1.40E-12

Table B4
Basic inputs and parameters for the descent flight phase for four reference aircraft [15].

Size Category		η_0	η_1	η_2	η_3	η_4	η_5	ϑ_0	ϑ_1	ϑ_2	ϑ_3	ϑ_4	ϑ_5
Small twin-aisle	JetA	332.8356	0.000916	−7.59E-08	−1.43E-07	0.001056	0	1.097209	−2.57E-06	−1.72E-10	−2.57E-10	2.48E-06	0
	LH_2	119.488	0.000329	−2.72E-08	−5.13E-08	0.000379	0	1.097209	−2.57E-06	−1.72E-10	−2.57E-10	2.48E-06	0
Medium twin-aisle	JetA	545.5971	0.006117	−1.92E-07	−5.16E-07	0.001766	0	2.903191	2.69E-05	−9.87E-10	−2.40E-09	9.14E-06	0
	LH_2	195.8694	0.002196	−6.89E-08	−1.85E-07	0.000634	0	2.903191	2.69E-05	−9.87E-10	−2.40E-09	9.14E-06	0
Large twin-aisle	JetA	539.0678	0.00051	−5.61E-08	−1.37E-07	0.000632	0	1.742666	1.09E-05	−2.98E-10	−7.94E-10	2.69E-06	0
	LH_2	193.5253	0.000183	−2.01E-08	−4.92E-08	0.000227	0	1.742666	1.09E-05	−2.98E-10	−7.94E-10	2.69E-06	0
Very large aircraft	JetA	944.718	0.004279	−1.19E-07	−6.07E-07	0.000993	0	4.456552	1.83E-05	−4.85E-10	−2.46E-09	4.62E-06	0
	LH_2	339.1538	0.001536	−4.27E-08	−2.18E-07	0.000356	0	4.456552	1.83E-05	−4.85E-10	−2.46E-09	4.62E-06	0

Appendix C:. Input parameters for economic assessment section

.

Table C1
Price of hydrogen and jetA fuel in different pathways.

Pathway	Price (USD $/kg fuel)	Ref.
SMR	1.22	[41]
BG	3.73	[42]
CG	1.18	[43]
EEG	5.31	[44]
ERE	5.4	[44]
RTS	4.55	[45]
JetA fuel	0.8	–

Table C2
Price of fee used in the economic assessment.

Fees	Value	Fees	Value
Handling price	0.1	ATC factor	0.5
Landing price	0.01	Carbon price	0.08266 ($/kg)
NOx price	1.5 ($/kg)	Interest rate	0.03
Cockpit salary (2020)	175,000 ($/year)	Depreciation period	15 (year)
Crew salary (2020)	85,000 ($/year)	Residual value	0.1
Labour rate (2020)	25 ($/h)	Spares Airframe	0.06
Interest rate	0.08	Spares Engine	0.23
Insurance rate	0.0035	Profit margin aircraft	0.2

Data availability

Data will be made available on request.

References

[1] Airbus. Global Market Forecast 2024. 2024.
[2] Supporting European Aviation. Aviation Outlook 2050: air traffic forecast shows aviation pathway to net zero CO_2 emissions. 2022.
[3] Rostami S, Javadi K, Maleki A. Taking stock of the climate impact of the hydrogen pathways for the aviation sector by 2050. Energy Convers Manag 2025;325:119369. https://doi.org/10.1016/j.enconman.2024.119369.
[4] Soyk C, Ringbeck J, Spinler S. Revenue characteristics of long-haul low cost carriers (LCCs) and differences to full-service network carriers (FSNCs). Transp Res E Logist Transp Rev 2018;112:47–65. https://doi.org/10.1016/j.tre.2018.02.002.
[5] IATA. Airline Profitability Outlook Improves for 2024. 2024.
[6] Afonso F, Sohst M, Diogo CMA, Rodrigues SS, Ferreira A, Ribeiro I, et al. Strategies towards a more sustainable aviation: a systematic review. Prog Aerosp Sci 2023;137:100878. https://doi.org/10.1016/j.paerosci.2022.100878.
[7] Eaton J, Naraghi M, Boyd JG. Regional pathways for all-electric aircraft to reduce aviation sector greenhouse gas emissions. Appl Energy 2024;373:123831. https://doi.org/10.1016/j.apenergy.2024.123831.
[8] Guo R, Dong J, Wolleswinkel RE, De Vries R, Niasar MG. Electrical architecture of 90-seater electric aircraft: a cable perspective. IEEE Trans Transp Electrif 2024:1. https://doi.org/10.1109/TTE.2024.3517838.
[9] Lau JIC, Wang YS, Ang T, Seo JCF, Khadaroo SNBA, Chew JJ, et al. Emerging technologies, policies and challenges toward implementing sustainable aviation fuel (SAF). Biomass Bioenergy 2024;186:107277. https://doi.org/10.1016/j.biombioe.2024.107277.
[10] Wang B, Ting ZJ, Zhao M. Sustainable aviation fuels: Key opportunities and challenges in lowering carbon emissions for aviation industry. Carbon Capture Sci Technol 2024;13:100263. https://doi.org/10.1016/j.ccst.2024.100263.
[11] Bhatt AH, Zhang Y, Milbrandt A, Newes E, Moriarty K, Klein B, et al. Evaluation of performance variables to accelerate the deployment of sustainable aviation fuels at a regional scale. Energy Convers Manag 2023;275:116441. https://doi.org/10.1016/j.enconman.2022.116441.
[12] Dray L, Schäfer AW, Grobler C, Falter C, Allroggen F, Stettler MEJ, et al. Cost and emissions pathways towards net-zero climate impacts in aviation. Nat Clim Chang 2022;12:956–62. https://doi.org/10.1038/s41558-022-01485-4.
[13] Hoelzen J, Koenemann L, Kistner L, Schenke F, Bensmann A, Hanke-Rauschenbach R. H2-powered aviation – design and economics of green LH2

supply for airports. Energy Convers Manage: X 2023;20:100442. https://doi.org/10.1016/j.ecmx.2023.100442.
[14] Adler EJ, Martins JRRA. Hydrogen-powered aircraft: Fundamental concepts, key technologies, and environmental impacts. Prog Aerosp Sci 2023;141:100922. https://doi.org/10.1016/j.paerosci.2023.100922.
[15] Lynnette Dray. AIM 2015 documentation (v11). 2023.
[16] Khan MAH, Brierley J, Tait KN, Bullock S, Shallcross DE, Lowenberg MH. The Emissions of water vapour and NOx from modelled hydrogen-fuelled aircraft and the impact of NOx reduction on climate compared with kerosene-fuelled aircraft. Atmosphere (Basel) 2022;13:1660. https://doi.org/10.3390/atmos13101660.
[17] Schenke F, Hoelzen J, Bredemeier D, Schomburg L, Bensmann A, Hanke-Rauschenbach R. LH2 supply for the initial development phase of H2-powered aviation. Energy Convers Manage: X 2024;24:100797. https://doi.org/10.1016/j.ecmx.2024.100797.
[18] Yusaf T, Faisal Mahamude AS, Kadirgama K, Ramasamy D, Farhana K, A. Dhahad H, et al. Sustainable hydrogen energy in aviation – a narrative review. Int J Hydrogen Energy 2024;52:1026–45. Doi: 10.1016/j.ijhydene.2023.02.086.
[19] Hoelzen J, Silberhorn D, Zill T, Bensmann B, Hanke-Rauschenbach R. Hydrogen-powered aviation and its reliance on green hydrogen infrastructure – review and research gaps. Int J Hydrogen Energy 2022;47:3108–30. https://doi.org/10.1016/j.ijhydene.2021.10.239.
[20] Warwick N, Griffiths P, Keeble J, Archibald A, Pyle J, Shine K. Atmospheric implications of increased Hydrogen use. 2022.
[21] Cooper J, Dubey L, Bakkaloglu S, Hawkes A. Hydrogen emissions from the hydrogen value chain-emissions profile and impact to global warming. Sci Total Environ 2022;830:154624. https://doi.org/10.1016/j.scitotenv.2022.154624.
[22] Stalker L, Roberts JJ, Mabon L, Hartley PG. Communicating leakage risk in the hydrogen economy: lessons already learned from geoenergy industries. Front Energy Res 2022;10. https://doi.org/10.3389/fenrg.2022.869264.
[23] Bertagni MB, Pacala SW, Paulot F, Porporato A. Risk of the hydrogen economy for atmospheric methane. Nat Commun 2022;13:7706. https://doi.org/10.1038/s41467-022-35419-7.
[24] Lakshmanan S, Bhati M. Unravelling the atmospheric and climate implications of hydrogen leakage. Int J Hydrogen Energy 2024;53:807–15. https://doi.org/10.1016/j.ijhydene.2023.12.010.
[25] Paulot F, Paynter D, Naik V, Malyshev S, Menzel R, Horowitz LW. Global modeling of hydrogen using GFDL-AM4.1: sensitivity of soil removal and radiative forcing. Int J Hydrogen Energy 2021;46:13446–60. https://doi.org/10.1016/j.ijhydene.2021.01.088.
[26] Ocko IB, Hamburg SP. Climate consequences of hydrogen emissions. Atmos Chem Phys 2022;22:9349–68. https://doi.org/10.5194/acp-22-9349-2022.
[27] Lissys. The PIANO X aircraft performance model. 2017.
[28] Association of European Airliners. AEA Requirements. Bruxelles: 1989.
[29] Michael N. Beltramo ; Donald L. Trapp; Bruce W. Kimoto; Daniel P. Marsh. Parametric study of transport aircraft systems cost and weight. 1977.
[30] Michael JS. Hydrogen Aircraft Concepts & Ground Support. Cranfield University , 2000.
[31] Air Transportation Association of America. Standard method of estimating comparative direct operating costs of turbine powered transport airplanes. 1967.
[32] Nicolai LM, Carichner GE. Fundamentals of Aircraft and Airship Design. Blacksburg, Virginia: American Institute of Aeronautics and Astronautics, Inc.; 2010. Doi: 10.2514/4.867538.
[33] Lubitz W, Tumas W. Hydrogen: an overview. Chem Rev 2007;107:3900–3. https://doi.org/10.1021/cr050200z.
[34] Wei C, Undavalli VK, Perkins C, Heglas K, Oswald E, Gbadamosi-Olatunde OB, et al. Technical and economic assessment of cryogenic fuels for future aviation. Progress in Aerospace Sciences 2024:101053. Doi: 10.1016/j.paerosci.2024.101053.
[35] Tiwari S, Pekris MJ, Doherty JJ. A review of liquid hydrogen aircraft and propulsion technologies. Int J Hydrogen Energy 2024;57:1174–96. https://doi.org/10.1016/j.ijhydene.2023.12.263.
[36] Daniel Brewer G. Hydrogen aircraft technology. CRC-Press 1991.
[37] Dray LM, Krammer P, Doyme K, Wang B, Al Zayat K, O'Sullivan A, et al. AIM2015: Validation and initial results from an open-source aviation systems model. Transp Policy (Oxf) 2019;79:93–102. https://doi.org/10.1016/j.tranpol.2019.04.013.
[38] Koroneos C, Dompros A, Roumbas G, Moussiopoulos N. Life cycle assessment of kerosene used in aviation (8 pp). Int J Life Cycle Assess 2005;10:417–24. https://doi.org/10.1065/lca2004.12.191.
[39] Kurzawska-Pietrowicz P. Life cycle emission of selected sustainable aviation fuels – a review. Transp Res Procedia 2023;75:77–85. https://doi.org/10.1016/j.trpro.2023.12.010.
[40] Lee DS, Fahey DW, Skowron A, Allen MR, Burkhardt U, Chen Q, et al. The contribution of global aviation to anthropogenic climate forcing for 2000 to 2018. Atmos Environ 2021;244:117834. https://doi.org/10.1016/j.atmosenv.2020.117834.
[41] Oni AO, Anaya K, Giwa T, Di Lullo G, Kumar A. Comparative assessment of blue hydrogen from steam methane reforming, autothermal reforming, and natural gas decomposition technologies for natural gas-producing regions. Energy Convers Manag 2022;254:115245. https://doi.org/10.1016/j.enconman.2022.115245.
[42] Cook B, Hagen C. Techno-economic analysis of biomass gasification for hydrogen production in three US-based case studies. Int J Hydrogen Energy 2024;49:202–18. https://doi.org/10.1016/j.ijhydene.2023.07.219.
[43] Li J, Wei Y-M, Liu L, Li X, Yan R. The carbon footprint and cost of coal-based hydrogen production with and without carbon capture and storage technology in China. J Clean Prod 2022;362:132514. https://doi.org/10.1016/j.jclepro.2022.132514.
[44] Department of Energy. Hydrogen and Fuel Cells Program Record. 2019.
[45] Budama VK, Johnson NG, Ermanoski I, Stechel EB. Techno-economic analysis of thermochemical water-splitting system for Co-production of hydrogen and electricity. Int J Hydrogen Energy 2021;46:1656–70. https://doi.org/10.1016/j.ijhydene.2020.10.060.